INTERPRETATIONS OF THE SHORT WAVE-LENGTH AEROMAGNETIC ANOMALIES IN THE CHUNGOWA DEPRESSION, CHAD BASIN, NIGERIA

BY

SANUSI YUSUFU ABUBAKR

A THESIS SUBMITTED TO THE POST-GRADUATE SCHOOL AHMADU BELLO UNIVERSITY, ZARIA IN PARTIAL FULFILLMENT OF THE REQUIREMENT FOR THE AWARD OF A MASTER DEGREE IN APPLIED GEOPHYSICS

DEPARTMENT OF PHYSICS,FACULTY OF SCIENCE

AHMADU BELLO UNIVERSITY

ZARIA, NIGERIA

JULY 1999

DECLARATION

I declare that this thesis is an original research carried out by the author. It has not been presented elsewhere for the award of a higher degree.



SANUSI, Y.A.

CERTIFICATION

This thesis entitled " Interpretations of the short wave-lengths aeromagnetic anomalies in the Chungowa Depression, Chad Basin, Nigeria" by SANUSI YUSUFU ABUBAKR meets the regulations governing the award of the degree of Master of Science of Ahmadu Bello University, and is approved for its contribution to knowledge and literary presentation.

Prof. C. O. Ajayi
Chairman, Supervisory commitee

23/7/99
Date

Prof. S . B. Ojo
Member, Supervisory commitee

23/07/99
Date

Prof. I. B. Osazuwa
Head of Department.

23/9/99
Date

Prof. S. B. Ojo
Dean, Postgraduate School

15/05/00
Date

ACKNOWLEDGEMENTS

My sincere gratitude goes to Professor C. O. Ajayi who suggested and supervised the work to its logical conclusion. His strong and logical criticisms at the various stages of the work is well appreciated. My gratitude also goes to Prof. S. B. Ojo my co - supervisor for his comments and suggestions which helped immensely in improving the work. My heartfelt gratitude also goes to Prof.I.B.Osazuwa, the Head, Department of Physics for his moral, material support and also for his concern. I would also like to thank all the staff of the Geophysics Unit of the Department of physics for their various contributions during the course of the work.I also wish to thank my classmates and friends who contributed in one way or the other, during the course of the master's program and to my wife for her patience and understanding. The financial assistance of the Usmanu Danfodiyo University, Sokoto is hereby acknowledged.

ABSTRACT

Aero magnetic data over the Chungowa Depression, Chad Basin, Nigeria has been studied in this work. The area is bounded between Longitudes 11 ° 30" E and 13°00"Eand Latitudes 12° 00" N and 12° 30" N. The Aeromagnetic maps supplied by the National Geological Survey, Kaduna, were digitized along the N - S flight lines at intervals of 0.5 Km to recover the original aeromagnetic data. The aeromagnetic data was then continued upward using a fortran computer program to 2.0 Km above the flight elevation to determine the regional field. The residual field of interest was then obtained by subtracting the determined regional field from the total field.

Qualitative interpretation of the aeromagnetic field revealed that the study area is characterized by both high and low gradient anomalies trending mostly along the EW and ENE directions with few anomalies along the N - S direction. Two lineaments and three extended gradients were also observed in the Study area.

The graphical techniques of Pal (1985) and Stanley (1977) were used to interpret the short wavelength anomalies of interest. The 2 - D interpretation based on the Pal's (1985) method shows that these anomalies were caused by intrusives lying predominantly between the depths of 0.011 Km and 1.29 Km with the shallow depths probably caused by shallow bodies which could be lava flows. The interpretation also suggested three set of ranges of the magnetic susceptibility contrasts associated with the igneous intrusions based on which the intrusions were thought to be granites, basalts and acidic rocks. On the other hand interpretations based on the Stanley's (1977) method suggested that the short wavelength anomalies of interest were caused by igneous intrusions lying predominantly between

0.148 Km and 1.18 Km. The interpretation also suggested three set of ranges for the susceptibility contrasts associated with the igneous intrusions based on which the intrusions were thought to be basalts, granites and acidic rocks.

Some of the modeled bodies were found to lie at shallow depths which could be lava flows. The presence of the lava flows and the basaltic intrusions suggests a rift origin for the basin through which the rocks ascended as a result of volcanism.

DEDICATION

" To my late Parents "

TABLE OF CONTENTS

CONTENTS **PAGE**

Title page.....i

Declaration ii

Certification iii

Acknowledgement iv

Abstract v

Dedication vii

Table of Content viii

List of Tables xiii

List of Figures xiv

List of Appendices.....xv

CHAPTER ONE : INTRODUCTION

1.1 General Description Of The Study Area I

1.2 Previous Work In The Study Area 3

1.3 Aim and Scope of the Present Work 3

CHAPTER TWO :GEOLOGY OF THE STUDY AREA.

2.1 Introduction 5

2.2 Stratigraphy of the Chad Basin 5

2.2.1 The Bima Sandstone 5

2.2.2 The Gongila Formation 5

2.2.3 The Fika Shales 6

2.2.4 The Gombe Sandstone 7

2.2.5 The Kerri - Kerri Formation 7

2.2.6 The Chad Formation 7

2.2.7 Volcanic Activities 7

2.3 Geological Evolution Of The Chad Basin 7

2.4 Structural Geology 7

CHAPTER THREE :PRINCIPLES OF THE AEROMAGNETIC METHOD AND THE INTERPRETATION TECHNIQUES USED

3.1 Geomagnetism 13

3.2 The Main Field 13

3.2.1 The External Field 14

3.2.2 Variations in the Main Field 14

3.3 Elements of the Geomagnetic Field 14

3.3.1 The Vertical Field 15

3.3.2 The Horizontal Field 15

3.3.3 The Total Field 15

3.3.4 Determination Of The Direction Of The Total Field 15

3.4 Principles Of Exploration Geomagnetism 17

3.5 The Aeromagnetic Method 17

3.6 Interpretation Techniques Used. 20

3.6.1 Isolating The Short Wavelength Anomalies 20

3.6.2 The Upward Continuation Process 21

3.6.3 The Stanley's Method Of Interpretation 21

3.6.4 The Pal's Method Of Interpretation 29

CHAPTER FOUR: DATA ACQUISITION, ANALYSIS AND INTERPRETATION

4.1 Introduction 36

4.2 Qualitative Interpretation 37

4.3 Quantitative Interpretation 37

4.3.1 Interpretation Procedure For The Stanley's Method 39

4.3.2 Interpretation Procedure For The Pal's Method 40

4.3.3 Testing The Reliability Of The Interpretation Techniques.....45.

4.3.4 *Comparison of the results obtained after testing the realibility of the interpretation* techniques.....45

4.4 Typical Interpretations 48

4.4.1 Typical Interpretation Of anomaly A1 Using The Pal's Method 48

4.4.2 Typical Interpretation Of anomaly A1 Using The Stanley's Method 50

4.5 Summary Of The Findings Of Our study 51

CHAPTER FIVE : DEDUCTIONS, CONCLUSIONS AND RECOMMENDATIONS

5.1 Deductions. 52

5.1.1 Comparison Of The Two Sets Of Interpretations 52

5.1.2 Geological Implication Of The interpretations. 53

5.2 Conclusions. 55

5.3 Limitation Of The Present Work. 57

5.4 Suggestion For Future Work 57

References 58

5.3 Limitation Of The Present Work. 57

5.4 Suggestion For Future Work 57

References 58

LIST OF TABLES

TABLE **PAGE**

2.1 Stratigraphic Sequence In The Chad Basin

(N. E Nigeria, After Matheis, 1976) 6

4.1 The Coefficient C_F and angle θ_F Of equation 3.20 43

5.1 a Suggested Depths And Susceptibility Contrasts Of The Modeled Igneous

Intrusions In Our Study Area 54

5.1 b The Susceptibilities Of Some Types Of Rocks 54

LIST OF FIGURES

Figures		PAGE
1.1	Chad Basin And Surroundings	2
3.1	Elements Of The Earth's Magnetic Field	16
3.2	Schematic Diagram Of A Flux - Gate Magnetometer	18
3.3	Total Field and Continued Field at 0.5 Km above the flight elevation	22
3.4	Continued Field at 1.0 Km and 1.5 Km above the flight elevation	23
3.5	Continued Field at 2.0 Km above the flight elevation	24
3.6	Geometry Of The Truncated Plate Of a Geological Contact	25
3.7	The Section Across The Strike Of An Inclined Thick Dike of Infinite Depth Extent And Explanation Of The Notations For Target Parameters	31
4.1	Total Intensity Map Of The Study Area	38
4.2	Diagrammatical Procedure For The Stanley's Method	41
4.3	Diagrammatical Procedure For The Pal's Method	44
4.4	Diagram showing the Reliability Of The Interpretation Techniques	46
4.5	Interpretation Of Anomaly A1 of Profile L200	49

LIST OF APPENDICES

APPENDIX		PAGE
I	Interpretation Of Anomaly A2 and A3 Of Profile L201	60
II	Interpretation Of anomaly A4 and A5 Of profile L202	61
III	Interpretation Of anomaly A6 and A7 Of profile L203	62
IV	Interpretation Of anomaly A8 of Profile L203	63
V	Interpretation Of anomaly A14 of profile L216	64
VI	Interpretation Of anomaly A19 and A20 Of Profile L219	65
VII	Interpretation Of anomaly A21 Of Profile L220	66
VIII	Interpretation Of anomaly A28 Of Profile L225	67
IX	Interpretation Of anomaly A29 Of Profile L226	68

CHAPTER ONE

INTRODUCTION

1.1 General Description of the Project Area

The Chungowa depression which is the area studied in this work, lies within the Nigerian sector of the Chad Basin. It is bounded by longitudes 11° 00″E and 13° 30"E and latitudes 12° 00″N and 12° 30″N. (Fig 1.1).

The Chad basin is the largest area inland drainage in Africa occupying about 230,000 Km^2 in the central sahara and southern Sudan (Barber, 1965). According to Matheis (1976), about one-tenth of the basin is situated in the north-eastern part Nigeria, where the western limit is formed by water divide between Niger and Chad drainage systems and the southern limit by the divide between Chad and Benue drainage systems.

Within Nigeria, the altitude of the basement falls to about 530 m at the western margin to about 300 m within the lake Chad along a long distance of about 240 Km (Matheis, 1976). This indicates a gentle slope towards Lake Chad. This generally low lying topography is interrupted by channels which extend for many kilometers (Matheis, 1976). Hydrologically, the Nigerian rivers within the basin generally drain northwards towards Lake Chad, within broad shallow valleys which only retain surface water after the heaviest rains (Matheis, 1976). The basin is of particular interest because of its proximity and possible structural relationship with Benue trough and also because of the economic implications of the iron formations found in a number of boreholes found in the basin.

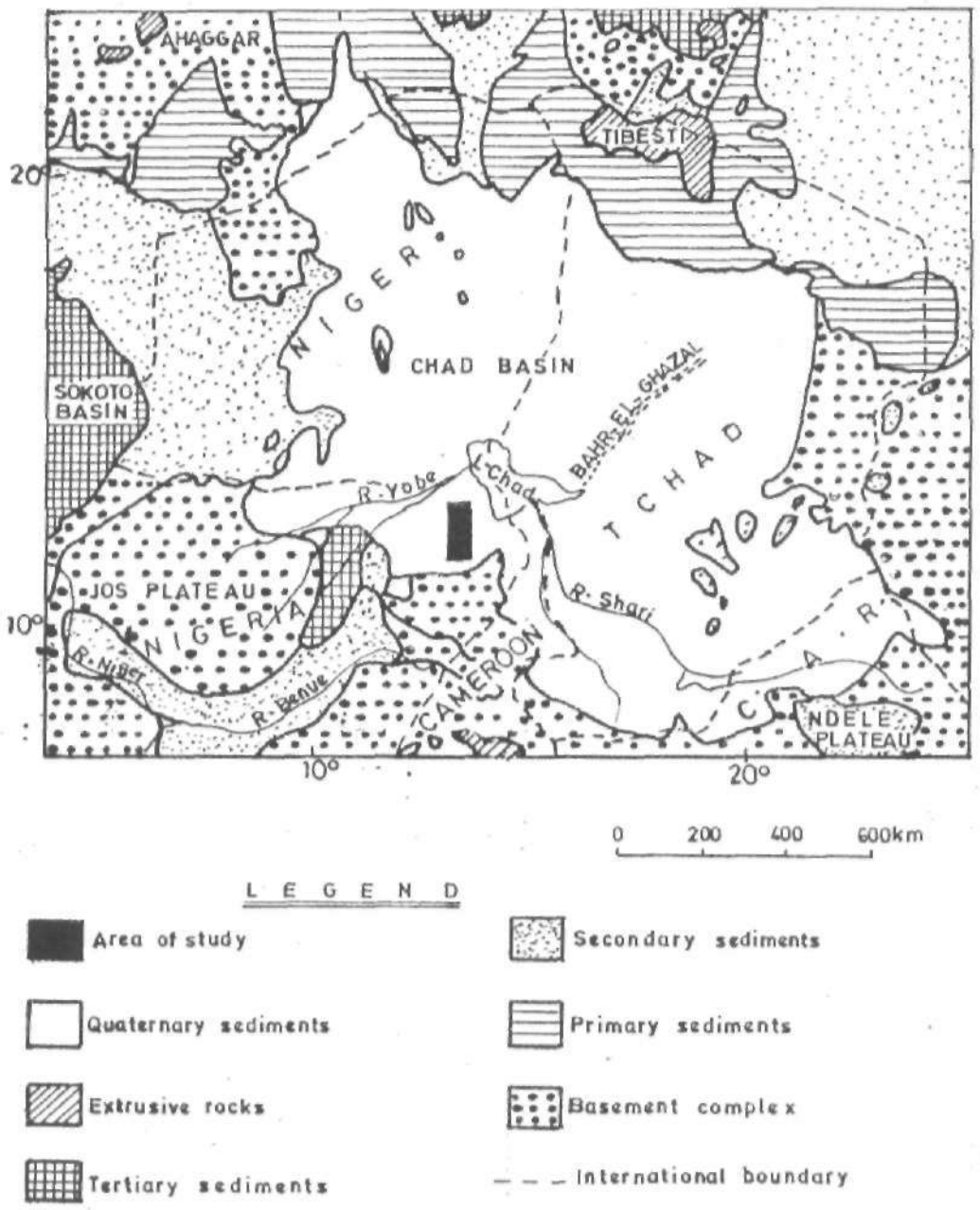


FIG.1.1. CHAD BASIN AND SURROUNDINGS (After Barber W. 1965)

1.2 PREVIOUS WORKS IN THE STUDY AREA

In 1960, Cratchley carried out a gravity survey of the southern part of the basin from which a Bouguer gravity map of a large fraction of the Nigerian portion of the Chad basin was compiled. The compilation was done by the Overseas Geological surveys and the map was incorporated into the Bouguer gravity map of Nigeria produced by Ajakaiye and Burke (1972). Also, Torkaski (1973), in searching for the possibility of the Chad oil in Nigeria, indicated the possibility of oil and gas in the basin. He further suggested a geophysical study of the basin. Also Yusuf (1990) carried out a detailed interpretation of the aeromagnetic data over parts of the Upper Benue trough which included part of our study area and obtained a depth to basement of about 2.0 Km for that part of the trough. Recently, the borehole logs of some recently drilled oil wells in the in the Nigerian section of the Chad basin intercepted several layers of hitherto unknown igneous intrusions which can act as structural traps for oil or channels for the evaporation of the accumulated oil (Ajayi and Nkereuwem 1992). Their interpretation of the broad or long - wavelength anomalies of an area containing the present study area based on Werner deconvolution solutions by Ajayi and Nkereuwem (1992) identified the locations of these intrusions and the gross thickness of the sediments within the area of our study which has a maximum value of 4 km. However the identified volcanic intrusions were not quantitatively modeled or interpreted. Hence the need for this work.

1.3 AIM AND SCOPE OF THIS WORK.

As stated above, the work of Ajayi and Nkereuwem (1992) was directed at interpreting

the gross structure of the basement below the flight lines over the Chungowa depression. As such the study did not interpret the relatively localized anomalies which they considered were due to the igneous intrusions suggested by the Werner profiles. Thus the present work is primarily embarked upon to interpret this localized or very short-wavelength anomalies. The graphical methods of Stanley (1977) and Pal (1985) were used for these interpretations due to the fact that the causative bodies for the anomalies of interest are thought to be dike - like bodies which these methods are good for. The anomalies of interest in this work are the short wave-length anomalies with widths not greater than 5 Km, which are believed to originate from the dike bodies and may be of interest for those exploring for oil/ petroleum in the basin. This is so because according to Ajayi and Nkereuwem (1992), these volcanic intrusions (dikes) might have acted as structural traps for hydrocarbons or source of heat for the evaporation of the hydrocarbons. The role in which they play, that is either as a trap or as a trap or as a heat source, depends on the relative ages of the hydrocarbons, if any, and the volcanic. As the approximate shape,sizes and the magnetic parameters of the magnetic intrusions are needed, these two interpretation techniques are considered to be sufficient.

CHAPTER TWO

GEOLOGY OF THE STUDY AREA

2.1 INTRODUCTION

The Chad basin which contains the Chungowa Depression cover parts of Nigeria, Niger, Chad and Cameroon. A map showing the geology and the extent of the basin in Nigeria, including the study area is shown in fig 1.1.

The area is covered by sediments which gently dip towards lake Chad and may therefore be classified as a covered shield area (Howell, 1959). The Chad basin is covered mainly by deposits known as Chad formation (Carter et.al., 1963). The crystalline rocks , which outcrops around the margin of the basin, consists of granite and flows of basalt (Barber, 1965).

2.2 STRATIGRAPHY OF THE CHAD BASIN

The stratigraphic sequence of the Chad basin consists of six formations namely the Chad formation, the Kerri-Kerri formation, the Gombe sandstone, the Fika shales, the Gongila formation and the Bima sandstone. The sequence is represented diagrammatically in table 2.1

Table 2.1: Stratigraphic sequence in the Chad Basin (N.E. Nigeria, After Mathias, 1976)

Age	Formation	Environment
Pleistocene	Chad Formation	Lacustrarine strata
Paleocene	Kerri-Kerri Formation (Unconformity)	Continental strata
Maestrichtion	Gombe sandstone	Estuarine-Deltaic strata
Senonian	Fika Shales	Marine strata
Turonian	Gongila Formation	Marine-Estuarine strata
Cenomanian	Bima Sandstone (Unconformity)	Continental Strata
Pre-Cenomanian	Basement complex	

2.2.1 THE BIMA SANDSTONE

This formation of probably Upper Aibian to Lower turonian age, (Matheis, 1976) .It outcrops both in the Chad basin and the Upper Benue basin but the thickness of the formation is much reduced along the Zambuk ridge separating the two basins (Matheis, 1976).

The Bima sandstone directly overlies the crystalline basement unconformably and varies in thickness from 100 m to over 3000 m (Matheis, 1976). The Bima sandstone probably resulted from the weathering of the granites of the Jos Plateau (Matheis, 1976).

2.2.2 THE GONGILA FORMATION

This formation is a transitional sequence between the purely continental Bima sandstone and the marine Fika shales which has a maximum thickness of about 500 m (Matheis, 1976). Numerous ammonites of Lower Turonian age are present (Reyment, 1956,

1965: Carter et. al., 1963).

2.2.3 THE FIKA SHALES

This are marine shales of Upper Turonian to Senonian age (Matheis, 1976). The Fika shales consists of blue-black shales, occasionally gypsiferous with thin limestone intercalations (Matheis, 1976). Fish and reptile remains obtained in them suggests Turonian to Maestrichtian age (Carter et.al., 1963).

2.2.4 THE GOMBE SANDSTONE

The Gombe Sandstone is a sequence of estuarine and deltaic sedimentation, best developed in the south-western portion of the basin, where a thickness of at least 350 m has been reported (Matheis, 1976). This formation gets thinner towards Lake Chad (Matheis, 1976). The Gombe Sandstone is not strongly folded and does not show the east- west trends which are imposed on the earlier Formations. The lower beds are characterized by mudstones and ironstones, while the middle part of the basin is composed of well- bedded sandstone and siltstones (Matheis, 1976). Towards the top sequence, cross- bedded sandstones are present (Matheis, 1976). The dating of the Gombe sandstone through palynological methods suggests Upper Maestrichtian to Pleistocene age.

2.2.5 THE KERRI-KERRI FORMATION

This formation rests unconformably on the folded Cretaceous sediments. It consists of a continental sequence of sediments dipping north-east beneath the Chad basin (Matheis,

1976). Drilling has proven that these sediments are wedged out between Maiduguri and the Damaturu - Gashua road (Matheis, 1976). The Kerri - Kerri formation appeared to have been derived from a terrain of Cretaceous sedimentary rocks whose relief was most subdued than the topography of the Bima sandstone times (Carter et. al., 1976). From palynological data a pliocene age has been suggested (Matheis, 1976).

2.2.6 THE CHAD FORMATION

This formation is a variable sequence that includes all the Quaternary sediments of lacustrine origin underlying the surface deposits over a vast area of about 15,000 Km^2 in Kano, Borno ,Yobe and Bauchi states. Within Nigeria, the Chad formation is exposed only on the southwestern margin of the basin and is essentially an argillaceous sequence in which the inpersistent arenaceous horizons occur (Matheis ,1976). The dating of the Chad formation was based on the vertebral remains of Lower Pleistocene and may also include deposits of Pliocene age (Barber and Jones, 1960).

2.2.7 VOLCANIC ACTIVITIES

Volcanic rocks are widely distributed in the north - eastern part of Nigeria. The youngest and more important phase of the activity occured during the Mid - Tertiary to recent time (Matheis, 1976).

The volcanic activity that had taken place in the Nigerian portion of the Chad basin is confirmed by the volcanic rocks that had emerged through the Chad formation in the Shari Delta in the Chad republic (Barber, 1965). The intrusions are classified into younger and older

series. The older intrusives consists mostly of entirely granites while the younger consists of principally granite and synetic and dia-basis types with numerous dike associated rocks (Barber, 1965).

2.3 GEOLOGICAL EVOLUTION OF THE CHAD BASIN

The geological history of the Chad basin in Nigeria began during the Upper cretaceous, probably Uppermost Albian (Matheis, 1976). During this period, continental sandstone consisting of the Bima sandstone were deposited uncomfortably on the pre - cambrian basement mainly to the south - west margin of the basin (Barber, 1965). These events were later followed by an extensive transgression and a mixed limestone/ shale sequence was deposited. The limestone/shale beds (Gongila formation) are overlain by over 530 m of marine shales (Fika formation) of turonian to senonian age. An estuarine - deltaic environment is thought to have prevailed towards the end of the Cretaceous (Maestrichtian), at which the Gombe sandstone was deposited with intercalations of siltstones, shales and ironstones (Furon, 1963). These sediments hardly extend far east into the Chad basin, but they probably attained a thickness of over 320 m where they occur (Matheis, 1976).

A period of folding occured at the end of the Cretaceous, so that the Cretaceous beds were folded into a series of synclines and anticlines that were later partly eroded creating an erosional unconformity at the base of the tertiary deposits.

The Kerri - Kerri formation, which does not extend far east into the Chad basin was deposited during the paleistocene. The Chad Formation was deposited unconformably on the Kerri - Kerri Formation and the older shales belonging to the Turonian to Senonian age.

The Chad Formation has been dated as Quaternary on the basis of the finding of the jaw of Hippopotamus Imaguncula Hopwood, in a hand dung well at a depth of 60 m (Durotoye, 1976). The dating indicated Lower pleistocene age but a considerable thickness of the Chad Formation below the dated level suggested that the Formation may also include deposits of Pliocene age (Barber, 1965). In the more recent times, dune sands accumulated in the Chad basin and several ancient dune systems may be identified. River alluvium and deltaic and lagoonal clay - flats that cover wide areas to the south and south - west of lake Chad are the youngest deposits (Matheis, 1976).

2.4 STRUCTURAL GEOLOGY

The earth movements and the recent climatic changes that have affected the Chad Basin may be summarized as follows:-

Late cretaceous

(i) Deposition of sandstone, Limestone and clays.

Close of Cretaceous

(ii) Secular elevation of the whole area, accompanied by folding and fracturing of the crust.

Early eocene

(iii) Intense erosion of the land surface, resulting in the complete denudation of the Cretaceous sediments over large areas.

Middle and Late eocene

(iv) Gradual subsidence, marked in its early stages by outflows of basalt in the south of the basin.

(v) Deposition of sediments; at first in the old river valleys and finally over the whole area.

Late eocene

(vi) Intermittent movements, the final results of which was the elevation of the whole area above the sea level; maximum elevation roughly along the watershed.

Eocene - Miocene

(vii) Erosion, during which the Kerri - Kerri Plateau and the Korode Hills were outlined and the eocene sediments in the north east of Nigeria and the adjoining French territory were almost completely denuded.

Miocene or Pliocene

(viii) Gradual subsidence, which was sufficiently marked in the northern Bornu, Katagum, and north - eastern Kano and the adjoining French territory to allow for the return of the sea.

(ix) Accumulation of drift over the greater part of the protectorate and the deposition of the Chad group in the sea.

Pliocene or Pleistocene

(x) General elevation of the whole area, the movement being accompanied by a gentle flexuring of the crust along the two sets of the axes at right angles. The Chad basin, lying between the various axes, was relatively depressed to least elevation occurring at Bodele.

(xi) Drainage of the Chad basin eastwards through the Bahr - el - Ghazal, with local erosion of the strata of the Chad group.

(xii) Uprise of the Chad - congo divide, cutting of the escape of the waters from the basin and causing swampy conditions in the Chad - Bodele area.

Recent

(xiii) Desiccation of the basin with the formation of the dunes, and the blocking of the other drainage channels.

(xiv) Comparatively humid climate of the present day. Drainage trending once towards the lowest point of the basin and leading to the formation of Lake Chad.

It will be observed that the Chad basin was an area of relative depression during all the earth - movements that have taken place since the eocene times

CHAPTER THREE

PRINCIPLE OF THE AEROMAGNETIC METHOD AND INTERPRETATION TECHNIQUES USED

3.1 GEOMAGNETISM

It has been known for more than three centuries that the earth behaves as a large, somewhat irregular, bar magnet. Extensive measurements of the magnetic elements have been made at sea because of their importance in connection with the use of magnetic compass for navigation and on land with the use of compass for surveying. Long-term studies of the magnetic elements have been made at magnetic observatories on land to study the slow changes in the geomagnetic field (Nettleton,1970).

As a result of these studies, it has been established that the geomagnetic field is composed of three parts namely; the main field ,the external field and the variation in the main field. Each of these components is briefly described below.

3.2 THE MAIN FIELD

This component of the Earth's magnetic field varies relatively slowly and is not constant in time. It is caused by an internal source, the mechanism of which several hypothesis have been put forward to account for. The most probable theory is that it is caused by electric current circulating in the outer core. The outer extends from a radius of 1300 km to 3500 km and is assumed to be a combination of iron and nickel; both of which are good conductors of electricity. The magnetic source is thought to be a self excited dynamo, in which a highly

conductive fluid moves in a complex mechanical motion, while the electric current, probably caused by chemical and thermal variation flow it. The combination of the motion and the current creates a magnetic field.

Laboratory test have shown that the dynamo source may be a valid explanation and may also account for certain secular variations which are known to have occured in the earth's magnetic field.

3.2.1 THE EXTERNAL MAGNETIC FIELD

This is a small fraction of the main field which varies rapidly, partly randomly and partly cyclically. The range of the daily variations in the vertical intensity may be as great as 100 gamma (Nettleton, 1970). The field originates outside the earth and is associated with the electric current in ionised layers of the outer atmosphere (Telford et. al., 1976).

3.2.2 VARIATIONS IN THE MAIN FIELD

This is usually, but not always, much smaller than the main field. It is relatively constant in time and place and is caused by the local magnetic anomalies in the near surface of the earth (Telford, 1976).

3.3 ELEMENTS OF THE GEOMAGNETIC FIELD

The geomagnetic field consists of three elements namely the vertical field, the horizontal field and the total fiield. Each of the elements is briefly discussed below.

3.3.1 THE VERTICAL FIELD

The intensity of the magnetic force at any point is denoted by F and its vertical component is called the vertical field. It is denoted by a letter Z or V and is reckoned positive downward as shown in fig 3.1. It is given the relation Z = F Sin I. (Where I is the inclination).

3.3.2 THE HORIZONTAL FIELD

The horizontal component of the magnetic force at any point is called the horizontal field and is always positive. It has two components X and Y which are considered positive in the north and east respectively as shown in fig 3.1. The horizontal field and its component are given by the following relationships $H = F \text{ Sin } I$, $H = F \text{ Cos } I$ and $Y = H \text{ Sin } D$ (where D is the declination).

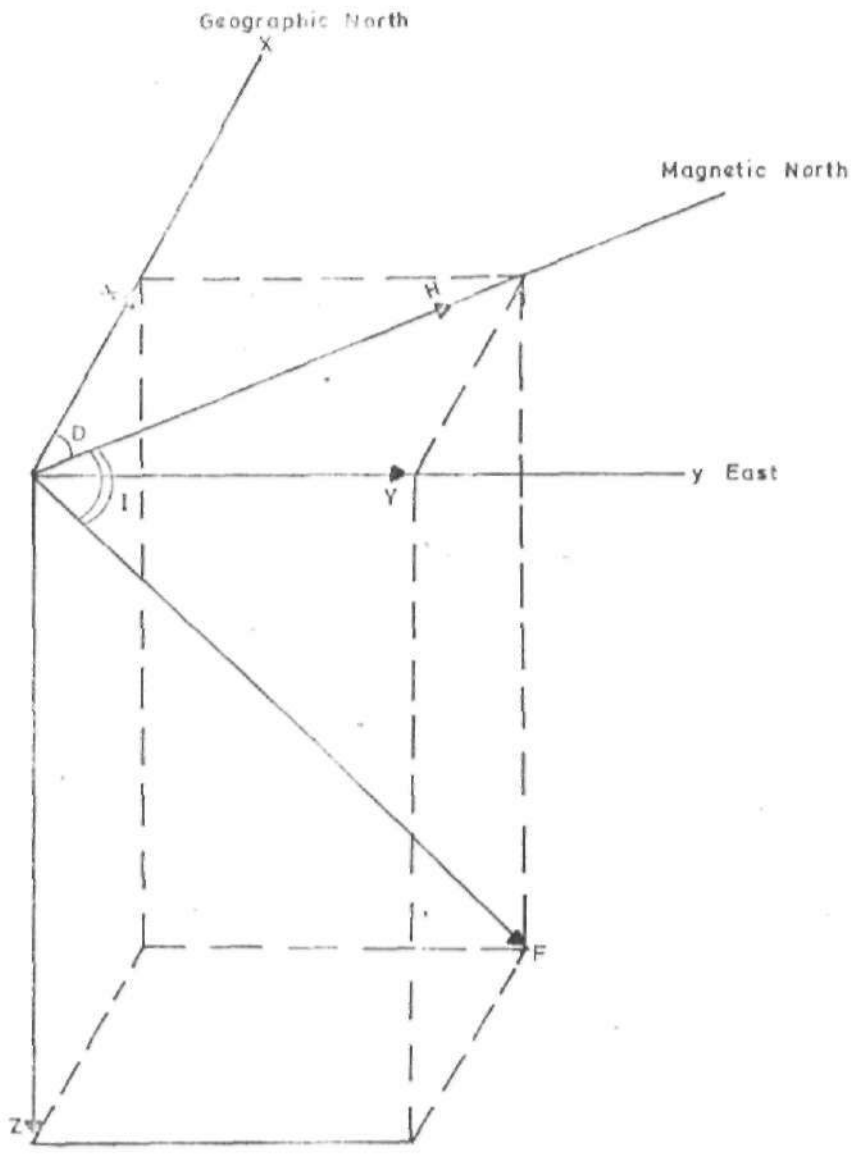
3.3.3 THE TOTAL FIELD

The algebraic sum of the vertical field and the horizontal field is the total field at that point as shown in fig 3.1. It is given by the following relationships:

$$F^2 = H^2 + Z^2 = X^2 + Y^2 + Z^2.$$

3.3.4 DETERMINING THE DIRECTION OF THE MAIN FIELD.

If a steel needle, not previously magnetised, could be hung at its center by a thread so that it were free to orient itself in any direction in space, at most points on the earth surface it will assumme neither horizontal nor in line with the geographic meridian. This orientation is the direction of the earth's total magnetic field at that point. The magnitude of this field, F, the



F = Total Magnetic Intensity
X = The North Component of F
Y = The East Component of F
Z = The Vertical Component of F
H = Total Horizontal Component
D = Angle of Declination
I = Angle of Inclination

FIG.3.1 ELEMENTS OF THE EARTH'S MAGNETIC FIELD

inclination of the needle from the horizontal, I, and its declination, D, the angle it makes with geographic north, completely defines the magnetic field.

3.4 PRINCIPLES OF EXPLORATION GEOMAGNETISM

The earth's crust contains a reasonable amount of ferromagnetic minerals and crystalline rocks of igneous origin such as granite, basalt and gabbro which contains appreciable amount of minerals such as magnetite and haematite. The rocks thus have a weak magnetisation which influences the earth's magnetic field above the surface of the earth to an appreciable that could be detected by sensitive instruments.

Fig. 3.2 illustrates how the field is measured by elements of this type in a fluxgate magnetometer. Two parallel cores are alligned with their axes in the direction of the earth's field. Primary coils in series magnetise the two cores with the same flux density in opposite directions, since they wound oppositely round the opposite cores. The earth's magnetic field at a given instant reinforces the field set up by one of the coils and opposes the field of the other. Each of the coils has in addition a secondary wounding, the two secondaries being connected to a voltmeter that reads the difference between the two outputs.

The instruments used in exploration includes fluxgate, nuclear precission and optical magnetometers.

3.5 THE AEROMAGNETIC METHOD

The vast majority of the magnetic surveys that have been made over the world were carried out with airborne instruments. Expriment with airborne instruments were carried out

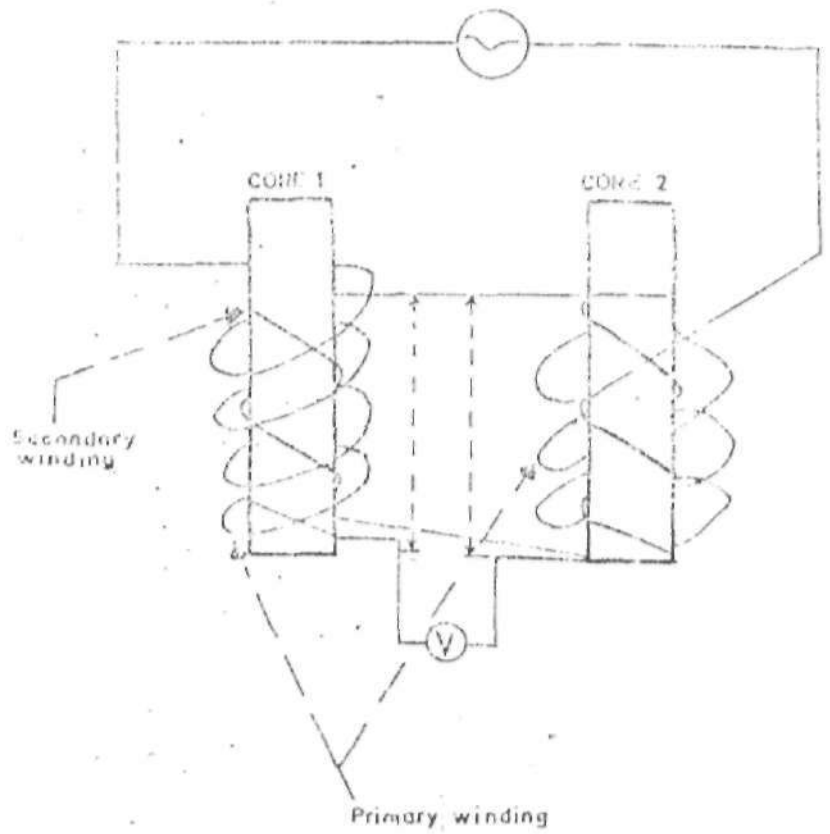


Fig 3-2 SCHE ATIC DIAGRAM OF A FLUX-GATE MAGNETOMETER.

as early as 1921 when a captive ballon was used for magnetic measurements over a known ore body in Sweden (Dobrin, 1976).

The airborne magnetomeler was later developed during the second world war for tracking submarines combined with radio locations for accurately locating aeroplanes. This constitutes one of the methods of modern geophysics by means of which magnetic surveys are made with great speed over land or water (Vacquier et al., 1951).

The instruments used for airborne magnetic surveys have greater sensitivities of about 1 - 5 gamma. Virtually all airborne detecting instruments measure total field (Dobrin, 1976; Telford et al., 1976).

The most usual procedure for placing the magnetometer head during flight is to tow the sensing element at the end of a cable at some distance behind the aeroplane, the detector is housed in streamlined cylindrical container known as the 'bird' which is about 25 - 30 m long and connected by a cable to the aeroplane or alternatively is mounted on a wing tip or slightly behind the tail.

For actual survey the the magnetometer is flown along a pre - selected set of lines, the altitude being kept as nearly vertical as possible and the height being continuoslly being recorded by an altimeter. Since both the magnetometer sensitivity and the earth's field may change due to instrumental drift and diurnal or more sudden variations, it is customary to make repeat readings during days flight pattern to record second readings at a number of intersections. The aircraft could be located at all times with respect to the ground position by a number of modern techniques, namely radio device systems, aerial photography, dobler system of navigation etc.

The data of the total magnetic field obtained during magnetic survey are presented on contour maps showing lines of equal strength of the anomaly or any of its componenets. The areal extent of the anomaly features roughly represents the extent of the contrast in the average content of the content of the ferro - magnetic minerals of the under - lying basement rocks.

The main advantage of aeromagnetic survey result from its great speed of surveying which reduces cost and also reduces the effect due to time variations in the magnetic field and instrumental drift. Erratic magnetic features near the surface of the earth which often consititutes a nuisance in ground work are reduced or completely eliminated by the height of the aircraft. In some cases, the elevation may be purposely chosen to favour certain geological structures of certain size and depth. Generally, no operational problems are associated with irregular terrain and also the survey could be made over water and other areas that are inaccessible for ground work.

The main disadvantage of airborne magnetic survey is the high initial cost for surveys over small areas for mineral exploration.

3.6 INTERPRETATION TECHOUES USED

3.6.1 ISOLATING THE SHORT WAVELENGTH ANOMALIES

An aeromagnetic map is charecterised by over abundance of details consisting of anomalies with large lateral extent and small lateral extent. The interesting anomalies resulting from the shallower features on the potential field maps are often masked by the effect of large scale deep seated structures. Thus, the first step in interpreting the short wavelength anomalies is to isolate them from the effect of the deep seated sources structures. The continuation

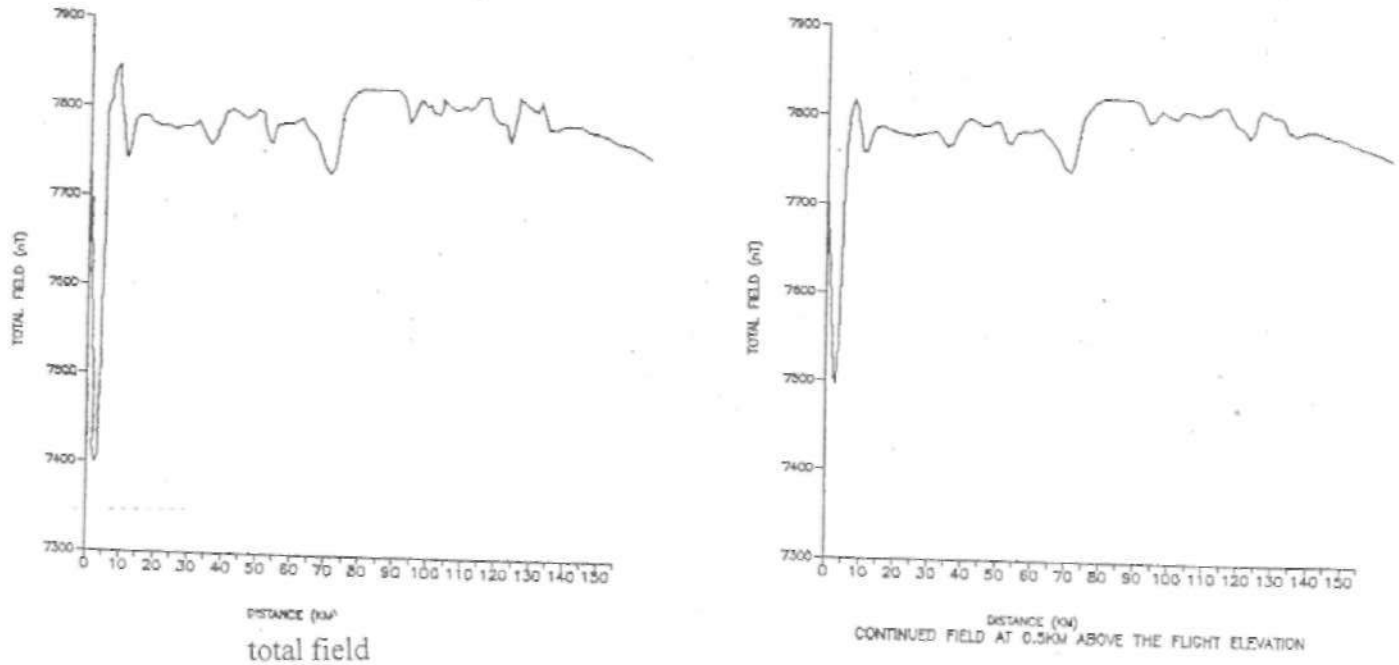
process described below is used to remove the long wavelength anomalies which are not of interest in this work.

3.6.2 THE UPWARD CONTINUATION PROCESS

This is a process in which the potential field data is mathematically projected upward to level surfaces above the datum level where the raw data was collected (Telford et al., 1976). It is usually done to simplify the appearance of the magnetic map by supressing the local features from the measured field. The potential field data used in this work was continued upward by using a Fortran computer program written by Prof S.B. Ojo of Physics Department, A.B.U Zaria. The program computes the values of the total magnetic field at various heights above the flight elevation using the fast Fourier transform technique. The total field was continued upward initially to a height of 0.5 Km and later to a height of 2.0 Km at regular intervals of 0.5 Km to supress the local features (Figs 3.3, 3.4 and 3.5a). However, at this height some traces of residuals were observed, hence the continued field was further smoothened to obtain a realistic regional (fig. 3.5b). The regional field was then substracted from the total field magnetic data to obtain the residual field of interest.

3.6.3 THE STANLEY'S METHOD OF INTERPRETATION

The method was introduced introduced by Stanley in 1977. It is a method of direct interpretation to determine the depth (d), dip (θ) and the susceptibility contrast (χ) values of contact and dyke bodies respectively. The method is applicable to both airborne and ground level data. The mathematical derivation of the method as given by Stanley (1977) is briefly discussed below.



total field

Fig. 3.3 Total Field and Continued Field at 0.5 Km above the flight elevation

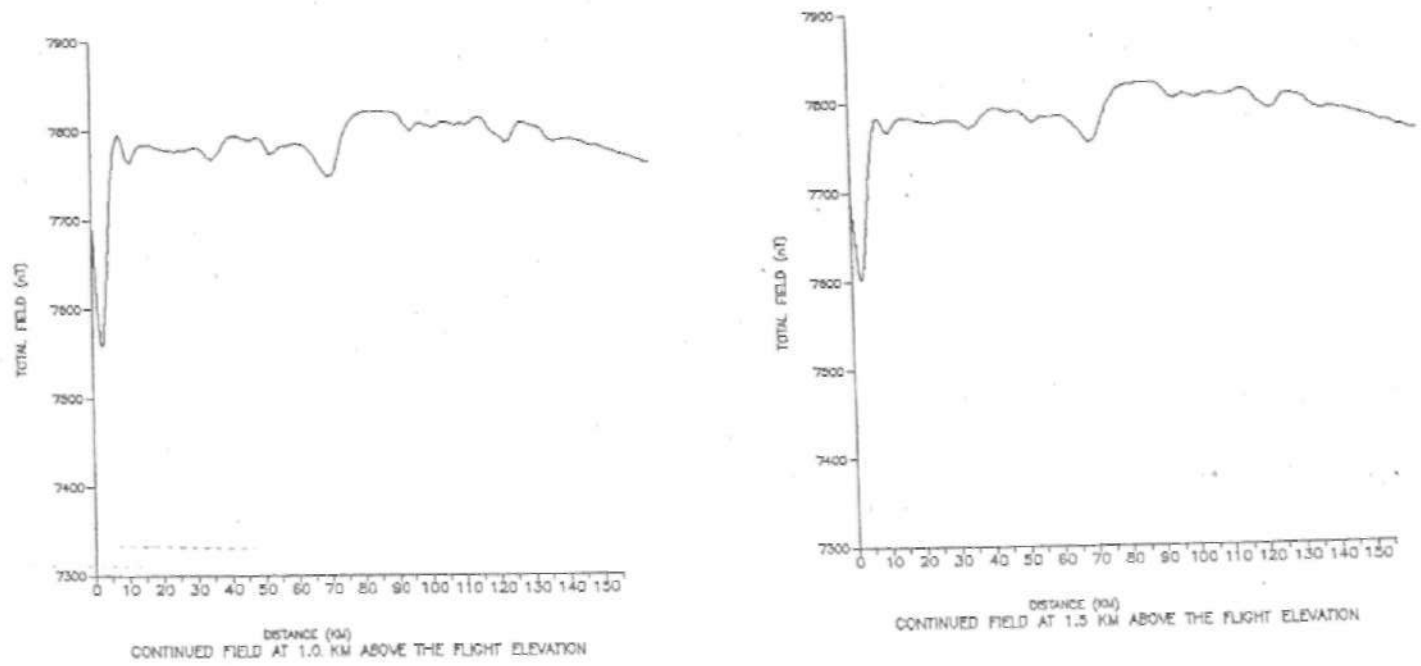


Fig 3.4 Continued Field at 1.0 Km and 1.5 Km above the flight elevation

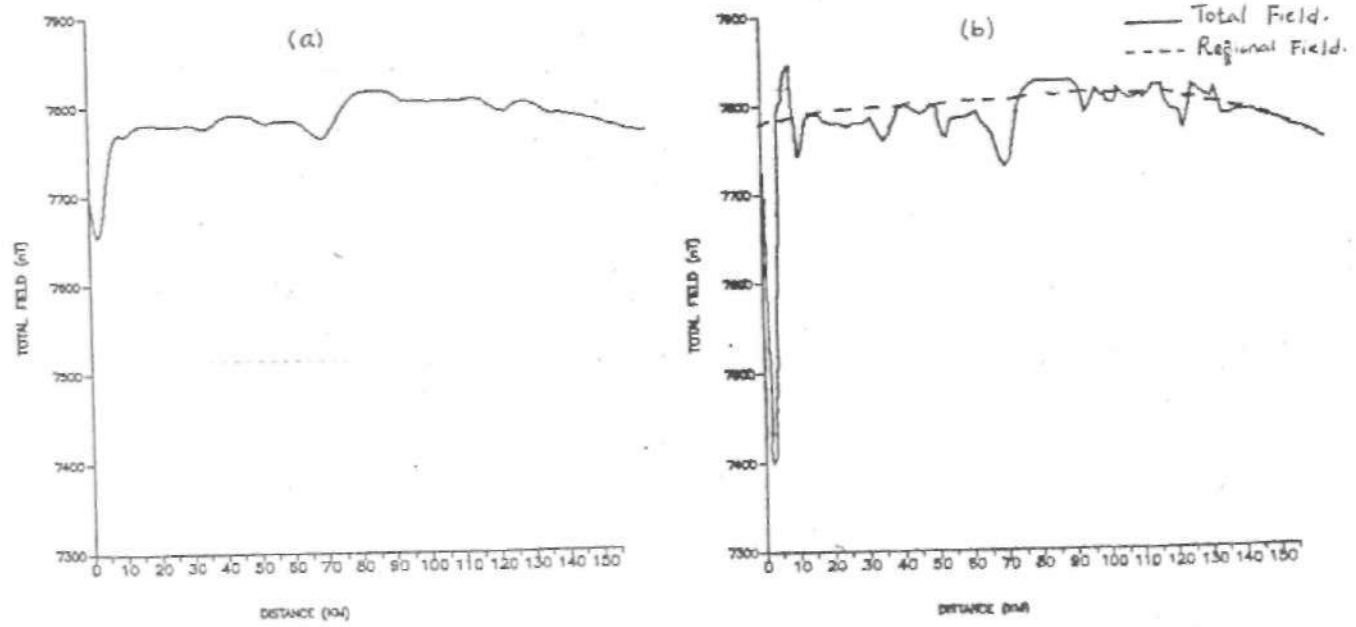


Fig 3.5a. Continued Field at 2.0 Km above the flight elevation

fig. 3.5b The total field with smoothened regional

MATHEMATICAL DERIVATION

The total magnetic field anomaly over a two - dimensional truncated plate (Fig 3.6) as given by Grant and West (1965) is

$$T(X) = \chi Tc\,(\sin\alpha\cos(\alpha - 2b)\ln((x-(D-d)\cot\alpha)^2 + D^2)/(x^2+d^2)) + 2\sin\alpha.\sin(\alpha-2b).(\arctan(x-(D-d)\cot\alpha/D) - \arctan(x/d)) \quad (3.1)$$

Where the parameters are explained in fig 3.6.

For convenience the following are introduced to simplify the above equation.

$$\phi = \alpha - 2b \quad (3.1a)$$

$$\theta = \arctan(x/d) \quad (3.1b)$$

$$r = (x^2+d^2)^{1/2} = d\sec\theta \quad (3.1c)$$

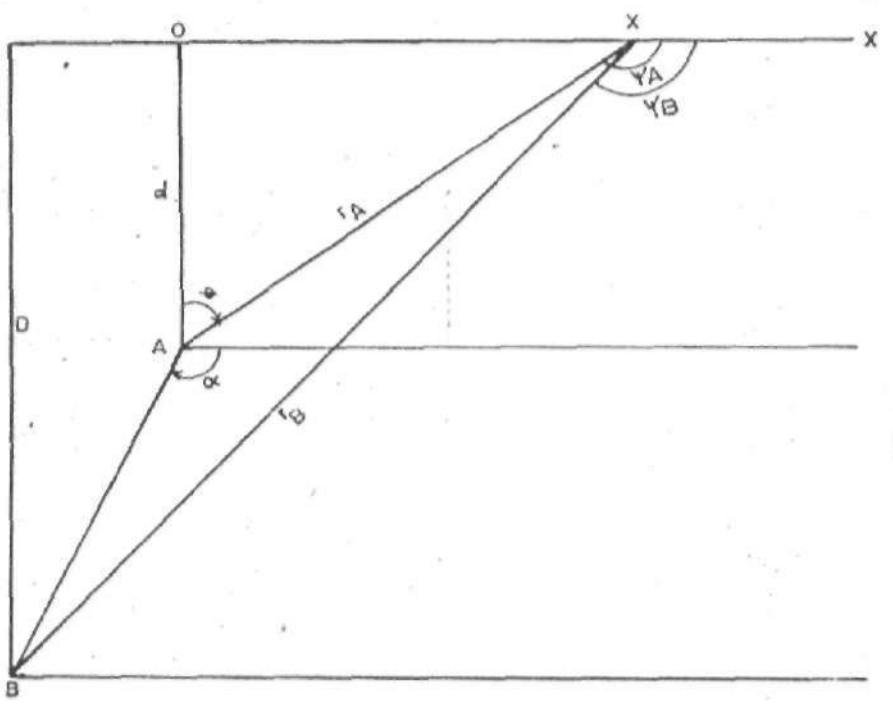
$$b = \arctan(\tan I/\sin\lambda) \quad (3.1d)$$

$$c = (1 - Cos^2 I\,Cos^2\lambda) \quad (3.1e)$$

$$K = 2\chi Tc\,Sin\alpha \quad (3.1f)$$

Where χ is the susceptibility contrast, I is the inclination and λ is the strike of the anomaly respectively. If we assume that the thickness is very great (D >>> d) then the truncated plate becomes a simple geological contact. In this case we differentiate equation (3.1) with respect to x and obtain

$$T_x(X) = -(K/r)\,Sin(\theta+\Phi) \quad (3.2)$$



NOMENCLATURE

A = Top shoulder of the truncated plate
B = Bottom shoulder of the truncated plate
X = Abscissa of profile with origin defined relative to the structure
d = Depth to the top of the structure
α = Angle of dip of the structure measured clockwise to the north
r_A = Radical distance of X to point A
r_B = Radical distance of X to point B
ϕ = Arctan (x/d)
γ_A = Angle at point X between X axis and line r_A
γ_B = Angle at point X between X axes and line r_B
D = Depth to the bottom of the structure.

FIG. 3.6. GEOMETRY OF THE TRUNCATED PLATE OF GEOLOGICAL CONTACT MODEL (After Stanley, 1977).

If a thin dyke is considered to be difference between the two contrasts situated ± W about the origin, then the equation becomes

$$T_x(X) = -(KW/r)\,Sin(\theta+\phi) \qquad (3.3)$$

The turning points of equations (3.2) and (3.3) can be found by equating the x derivative of each of the equation with zero. The maximum and the minimum of each are found to occur at x_M and x_m respectively where

$$X_M = -d\,(Sec\,\phi+Tan\,\phi) \qquad (3.4)$$

$$X_m = d\,(Sec\Phi-Tan\Phi)\,. \qquad (3.5)$$

By substituting equations (3.4) and (3.5) in equation (3.2), the values of the maxima (M) and the minima (m) of T (x) for a contact are given by

$$M = Kd/(X_M^2 + d^2) \qquad (3.6)$$

and

$$m = -Kd/(X_M^2 + d^2) \qquad (3.7)$$

Also the substitution of equations (3.4) and (3.5) in equation (3.3) gives the values of the turning points of T (x) over a thin dyke as

$$M = KWd/(X_M^2 + d^2) \qquad (3.8)$$

$$m = - KWd / (X_m^2 + d^2) \qquad (3.9)$$

By substituting x = 0 in equation (3.2) we get for a contact:

$$T_x(0) = (- K/d) \; Sin \; \Phi \qquad (3.10)$$

and for a thin dyke:

$$T_x(0) = - (KW/d) \; Sin \; \phi \qquad (3.11)$$

The x - position where the ordinate is zero is found by equating equation (3.2) or (3.3) to zero. In both cases of a contact and a thin dyke we obtain

$$X = - d \tan \phi \qquad (3.12)$$

Clearly, equations (3.4) through (3.12) are sufficient to solve for the unknown variables θ, d, K, and KW. The choice of which equation to use will depend on which of the characteristic points will be precisely determined from the profile.

Furthermore, equations (3.4) through (3.9) may be manipulated to obtain the following results.

$$M + m = (- K/d) \; Sin \; \phi \qquad (3.13a)$$

or

$$(KW/d) \; Sin \phi = T_x(0) \qquad (3.13b)$$

$$m = - KWd / (X_m^2 + d^2) \qquad (3.9)$$

By substituting x = 0 in equation (3.2) we get for a contact:

$$T_x(0) = (- K/d) \, Sin \, \Phi \qquad (3.10)$$

and for a thin dyke:

$$T_x(0) = - (KW/d) \, Sin \, \phi \qquad (3.11)$$

The x - position where the ordinate is zero is found by equating equation (3.2) or (3.3) to zero. In both cases of a contact and a thin dyke we obtain

$$X = - d \tan \phi \qquad (3.12)$$

Clearly, equations (3.4) through (3.12) are sufficient to solve for the unknown variables θ, d, K, and KW. The choice of which equation to use will depend on which of the characteristic points will be precisely determined from the profile.

Furthermore, equations (3.4) through (3.9) may be manipulated to obtain the following results.

$$M + m = (- K/d) \, Sin \, \phi \qquad (3.13a)$$

or

$$(KW/d) \, Sin \, \phi = T_x(0) \qquad (3.13b)$$

$$M - m = -K/d \text{ for a contact} \qquad (3.14)$$

and

$$M - m = KW/d \text{ for a thin dyke} \qquad (3.15)$$

$$(M + m/M - m) = Sin\,\phi \qquad (3.16)$$

$$X_M + X_m = -2d\tan\phi \qquad (3.17)$$

$$(X_M + X_m) / (X_M - X_m) = Sin\,\phi \qquad (3.18)$$

$$-X_M X_m - d^2 \qquad (3.19)$$

For most values of θ, both the maxima and the minima will be located in close proximity to the top of the structure, thus making this points immune from the neighbouring interference.

To determine the origin of the profile a straight line joining the maximum to the minimum cuts the curve at the origin (i.e x = 0)

3.6.4 THE PAL'S METHOD OF INTERPRETATION.

This is a direct method of interpretation of inclined thick dykes of finite extent to obtain the depth (d), the width (w), the dip (θ) and the susceptibility contrast (χ).

The mathematical analysis of the method as given by Pal (1985) is as follows:

Ascribing the magnetisation of a dyke of magnetic susceptibilty due exclusively to induction in the local geomagnetic field of strength F and inclination I and neglecting the demagnetisation effect, the analytical expression for ΔF, the magnetic anomaly at any point on the profile across the buried source can be written (Gay, 1963) as:

$$\Delta F = C_F \{ (\Phi_A - \Phi_B) \cos\theta_F + \sin\theta_F \ln(r_A / r_B) \}. \qquad (3.20)$$

The notations used in this equation are

a) ΔF is ΔZ, ΔH, or ΔT, the vertical, horizontal or the total field anomaly, depending upon what is measured. In this work ΔT was measured, hence ΔF is ΔT.

b) The expressions for the coeffients C_F and angle θ_F depend whether ΔF is ΔZ,ΔH or ΔT their values are summarized in table 4.1.

c) ϕ_A, ϕ_B, r_A, and r_B are functions of the dyke parameters h (depth of burial), b (semiapical width), and the x (the distance of field on the profile relative to the epicentral position x of the dyke) in the following manner:

$$\Phi_A = \tan^{-1}((x + b) / h), \qquad (3.21)$$

$$\Phi_B = \tan^{-1}((x - b) / h), \qquad (3.22)$$

$$r_A^2 = h^2 + (x + b)^2 \qquad (3.23)$$

and

$$r_B^2 = h^2 + (x - b)^2 \qquad (3.24)$$

d) the dyke parameters h, b, χ and X_0 are explained in fig 3.7

The ΔF profile of equation (3.20) has several characteristics which can be effectively used in the estimation of the source characteristics. First this profile has a characteristic maxima (M : X_M) and minima (m : X_m) points as long as θ_F approaches neither zero nor 180 degrees. The coordinate of these minima and maxima are determined by deriving an analytical expression for the horizontal gradient or ΔF_x profile (since $\Delta F = 0$ at $X = X_m$ or $X = X_M$).

Differentiating the two sides of the equation (3.20) with respect to x, we obtain the expression for ΔF_x as

$$\Delta F_x = (2bC_F / r_A^2 r_B^2)\ ((h^2 + b^2 - x^2)\ Sin\,\theta_F - 2xh\,Cos\,\theta_F) \qquad (3.25)$$

Hence, by setting $\Delta F_x = 0$ in equation (3.25)

$$X = X_M = -(h\,Cot\,\theta_F + R) \qquad (3.26)$$

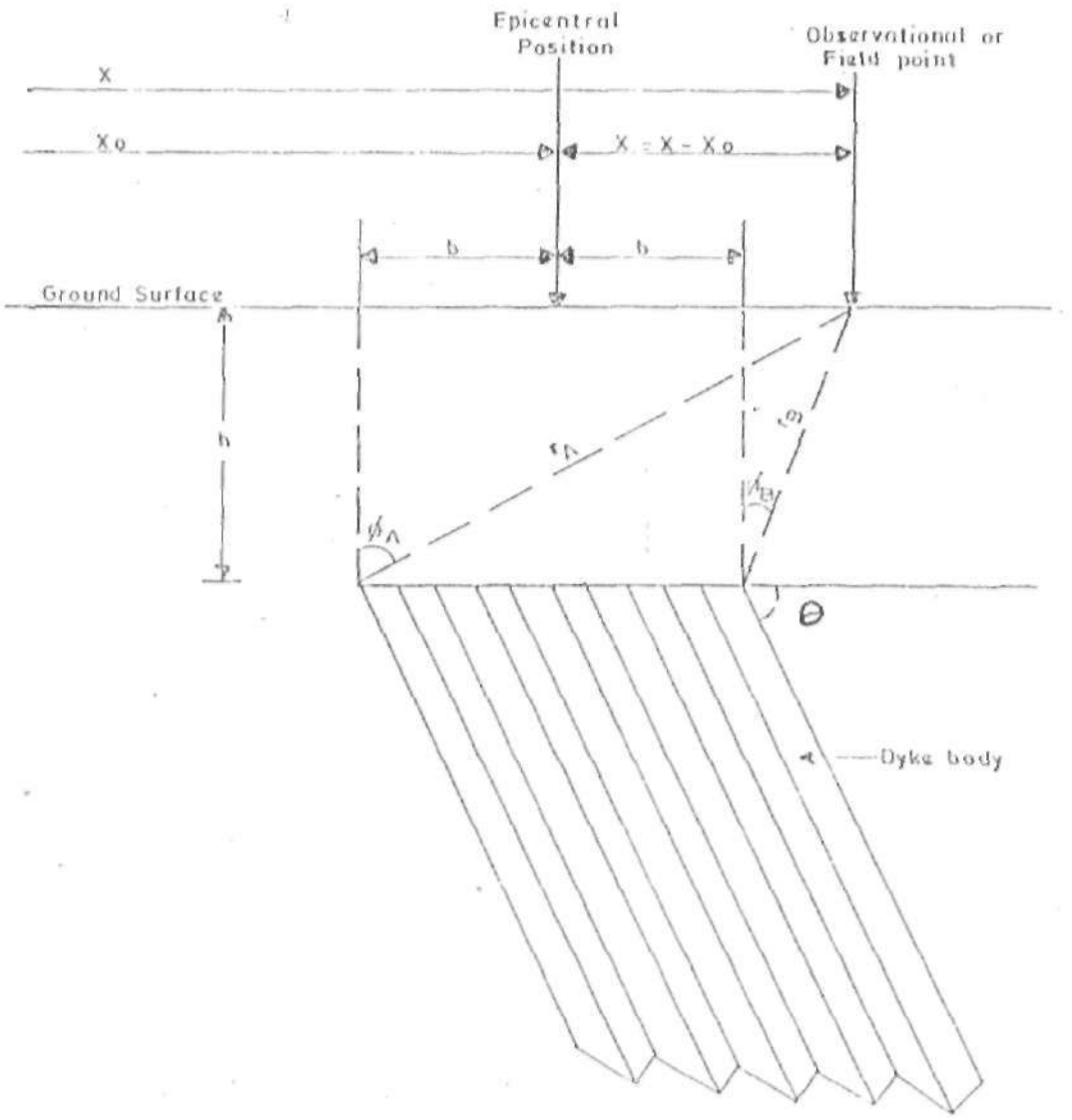
and

$$X = X_m = -(h\,Cot\,\theta_F - R) \qquad (3.27)$$

where

$$R = \sqrt{(b^2 + h^2\,cosec^2\theta_F)}$$

Since M = ΔF ($x = x_M$) and m = ΔF ($x = x_m$), equations (3.20), (3.26) and (3.27) yield



NOMENCLATURE

h = Depth of burial
b = Semiapical width
X = Distance of the field point on the profile relative to the epicentral position Xo of the dyke
ϕ_A, ϕ_B, r_A, r_B = Functions of dyke parameters h, b and X
Θ = Dip angle

FIG.3.7: THE SECTION ACROSS THE STRIKE OF AN INCLINED THICK DIKE OF INFINITE DEPTH EXTENT AND THE EXPLANATION OF NOTATIONS FOR TARGET PARAMETERS (After Pal (1985))

$$M = C_F (Cos\,\theta_F\, Tan^{-1} A_1 + (1/2) Sin\theta_F \ln(R - b)/(R + b)) \qquad (3.27a)$$

and

$$m = C_F (Cos\,\theta_F \tan^{-1} A_2 - (1/2) Sin\,\theta_F \ln(R - b)/(R - b)) \qquad (3.27b)$$

where

$$A_1 = b/(h\,\mathrm{cosec}^2\,\theta_F + R\,Cot\,\theta_F) \qquad (3.27c)$$

and

$$A_2 = b/(h\,\mathrm{cosec}^2\,\theta_F - R\,Cot\theta_F) \qquad (3.27d)$$

Likewise, the following expression for ΔF (0) is obtained by setting x = 0 in equation (3.20),

$$\Delta F(0) = 2C_F \cos\theta_F \tan^{-1}(b/h). \qquad (3.28)$$

and by comparing equations (3.27 c) , (3.27 d) and (3.28) we obtained

$$\Delta F(0) = M + m \qquad (3.29)$$

The epicentral $X = X_0$ or $x = 0$ is thus the coordinate on the distance axes at which the anomaly has the same value as the algebraic sum of maximum and minimum (because the signs of M and m are opposite this actually mean their difference). This is the second characteristic feature of the ΔF profile of equation (3.20). The third characteristic feature of the profile is

summarised in the following relations between the values of x_M and x_m and the dyke parameters h, b, and θ_F:

$$1/2\ (X_m + X_M) = -\ h \cot\theta_F \qquad (3.30)$$

$$1/2\ (X_M + X_m) = R = \sqrt{(b^2 + h^2\ \mathrm{cosec}^2\ \theta_F)} \qquad (3.31)$$

and

$$-\ X_m .\ X_M = (b^2 + h^2) = U^2 . \qquad (3.32)$$

Finally, since the positions x = 0 and $x = U = \sqrt{(|-x_M . X_m|)}$ are readily determinable, equations (3.25) gives the values of $\Delta F_x(0)$ and $\Delta F_x(U)$ as

$$\Delta F_x\ (0) = (2\ b\ /\ U^2)\ C_F\ \ Sin\ \theta_F \qquad (3.33)$$

and

$$\Delta F_x\ (U) = (-b/\ Uh)\ C_F \cos\theta_F . \qquad (3.34)$$

Equations (3.30), (3.31) , (3.33) and (3.34) then shows that the ratio ($\Delta F_x(0)/\ \Delta F_x(U)$) bears the following the relation with θ_F:

$$(\Delta F_x\ (0)\ /\Delta F_x\ (U)\ ) = (\ (X_m + X_M)\ /\ U)\ \tan^2\theta_F = B^2 . \qquad (3.35)$$

thus

thus

$$\theta_F = \pm \tan^{1} B \sqrt{(U/(X_m + X_M))} \qquad (3.36)$$

These characteristics of the observed magnetic profile ΔF and of its horizontal gradient ΔF_x can be thus used for estimating the values of the target or unknown parameters h, b, θ and θ_F.

CHAPTER FOUR

DATA ACQUISITION, ANALYSIS AND INTERPRETATION

4.1 INTRODUCTION

The data used in this work was obtained by digitizing three aeromagnetic maps(sheets 88, 65 and 43). The maps were supplied by the Geological Survey of Nigeria, Kaduna and were in half-degree sheets obtained from the aeromagnetic survey flown at a nominal flight altitude of 0.762 Km. Each map consists of twenty seven profiles each 2 Km apart oriented along the north-south flight lines labelled L200, L201, L202 ..... L226 respectively. The maps were compiled in 1975 by the Geological Survey of Nigeria and a regional correction based on the International Geomagnetic Reference Field (I.G.R.F) epoch date, 1st January, 1976 was included in all the maps.

Though the primary aim of this work is not to interpret the entire maps of the study area, nevertheless, the interpretation is divided into two parts the qualitative and the quantitative. In the qualitative interpretation, effort is made to describe the pattern of the aeromagnetic field over the study area and to infer from the magnetic data the presence of structures such as faults, lineaments etc in the area. On the other hand the quantitative interpretation was carried out to determine the source parameters such as depth, dip, widths and the susceptibility contrasts of the subsurface structures causing the aeromagnetic anomalies. The details of each of the two methods of interpretation are discussed below.

4.2 QUALITATIVE INTERPRETATION

A close inspection of the total intensity map of the study area (fig 4.1) shows prominent linear anomalies of both high and low gradients. Notable are the intense magnetic closures in the southern half of the study area. Most of the anomalies are trending along the EW and ENE directions .Three prominent long extended gradients are also observed to the east of Muti, directly to the north of Katti-Kime and Ngannu respectively. These long extended gradients usually represent major faults or shear zones according to Affleck or sharp contacts between two major shear zones. Magnetic anomaly closures associated with these high gradients could reflect the occurrence of highly magnetized intrusions which lie at shallow depths. The depth to basement is shallower in the southern half of the study area than in the northern half.

Two magnetic lineaments labeled AA' and BB' were observed on the total magnetic map. The lineament AA' could have been as a result of change in magnetization. This is informed by the change in magnetization on either side of the lineament. While lineament BB' could be as a result of faulting . This is due to the fact that long wavelength anomalies are observed on either side of the lineament.

4.3 QUANTITATIVE INTERPRETATION

Quantitative interpretation is usually embarked upon to determine the depth, width, dip and susceptibility contrasts of the subsurface structures causing the aeromagnetic anomalies. Several techniques have been developed to interpret dike bodies. In space domain Johnson (1969) and Won (1981) developed techniques in which iterative

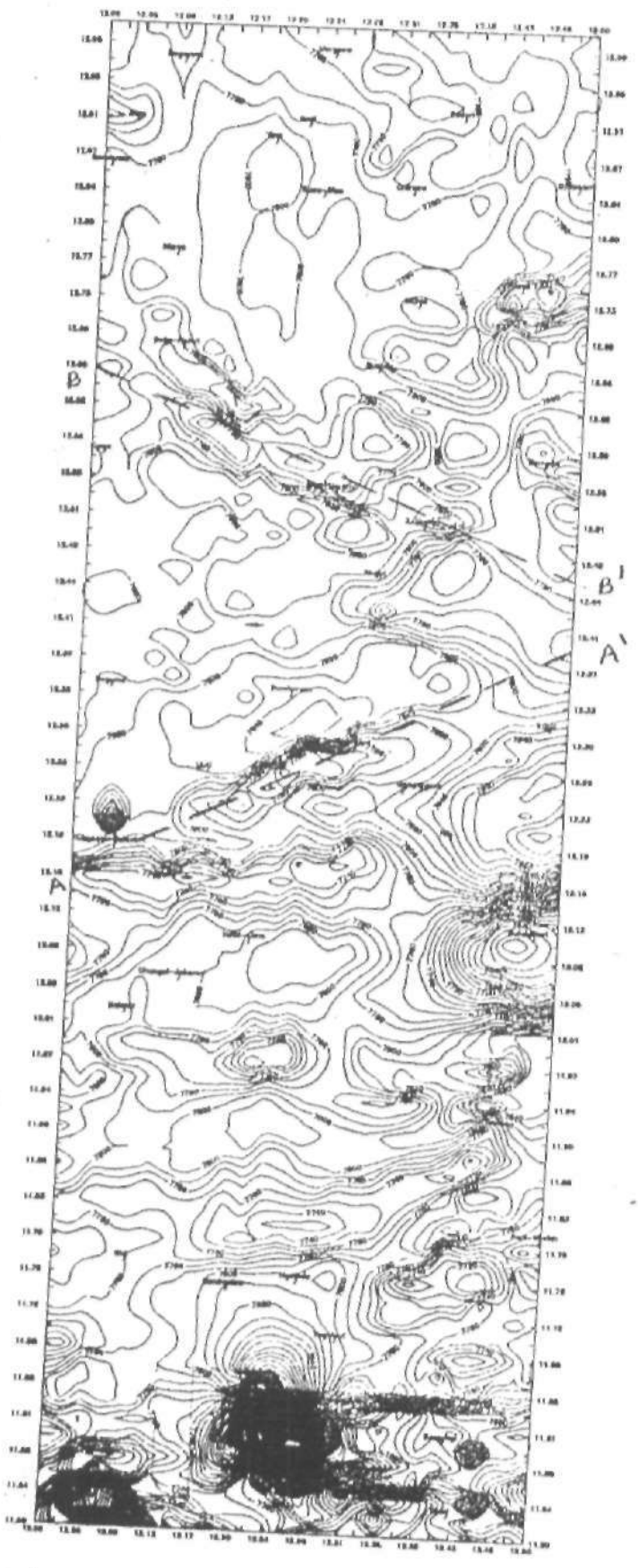


Fig. 4.1 Total Field Intensity map of the study Area.
(Contour Interval 10 nT)

computations are needed to obtain accurate estimates for the parameters of the source. The iterations make the techniques to be time consuming. Similarly,interpretation techniques in which an anomaly is compared with standard curves to obtain accurate estimates for the target (source) parameters have been developed (e.g. Gay, 1963) but they are also generally time consuming.

The methods of Pal (1985) and Stanley (1977) which are fairly simple and rapid to use have been used in this work due to their accuracies, time saving and ease of application. Both the Stanley's (1977) method and the Pal's (1985) method requires both the total field profile and it's derivative for its application. The Stanley's (1977) method work better for thin dikes while the Pal's (1985) method work better for thick dikes. The combined application of the two methods is expected to give all the parameters needed to interpret the causative dike-like body. It is worth mentioning here that a value of 0.7625 km was subtracted from each of the depth estimates determined so as to take care of the flight elevation. This makes the depth estimate to be with respect to the surface of the ground. Also some of the depth estimates for some of the anomalies were with a cosine correction factor as to take care of errors that might arise due to their strike directions not being perpendicular to the profiles (i.e the flight lines).

4.3.1 INTERPRETATION PROCEDURE FOR THE STANLEY'S METHOD

The procedure normally followed method in using the Stanley's method as given by the author Stanley (1977) are itemized below.

1). Noting the inclination of the field in the study area (I) and also the strike

angle (λ) of the aeromagnetic anomalies on the aeromagnetic map.

These values are normally used to determine the constants b and c respectively.

2) Locating the epicentral position of the anomaly (i.e x = 0). This is usually done by drawing a straight line joining the minima to the maxima of the anomaly curve. The point where this line cuts the curve locates the vertical axes of the anomalous body. Thus the corresponding coordinate of the vertical axes on the distance axis locates the centre of the anomaly. This enables the precise determination of the horizontal position of the maxima (x_M) and the minima (x_m) respectively (fig 4.2). The baseline which enables the precise determination of the minimum and the maximum of the anomaly is then constructed at a value M - T_x (0) above the minimum.

3) The four characteristic points i.e m, M ,X_m and X_M determined above are then used in equations (3.15), (3.16) and (3.19) to estimate the parameters K , ϕ and the depth to the top of the source (d) respectively.

4) With the values determined above, equations (3.1a) and (3.1f) are then used to estimate the dip angle (α) and the susceptibility contrast (χ) respectively.

The steps itemized above are illustrated in fig 4.2.

4.3.2 INTERPRETATION PROCEDURE FOR THE PAL'S METHOD

The procedure normally followed in using the Pal's method as given by the author Pal (1985) are as itemized below.

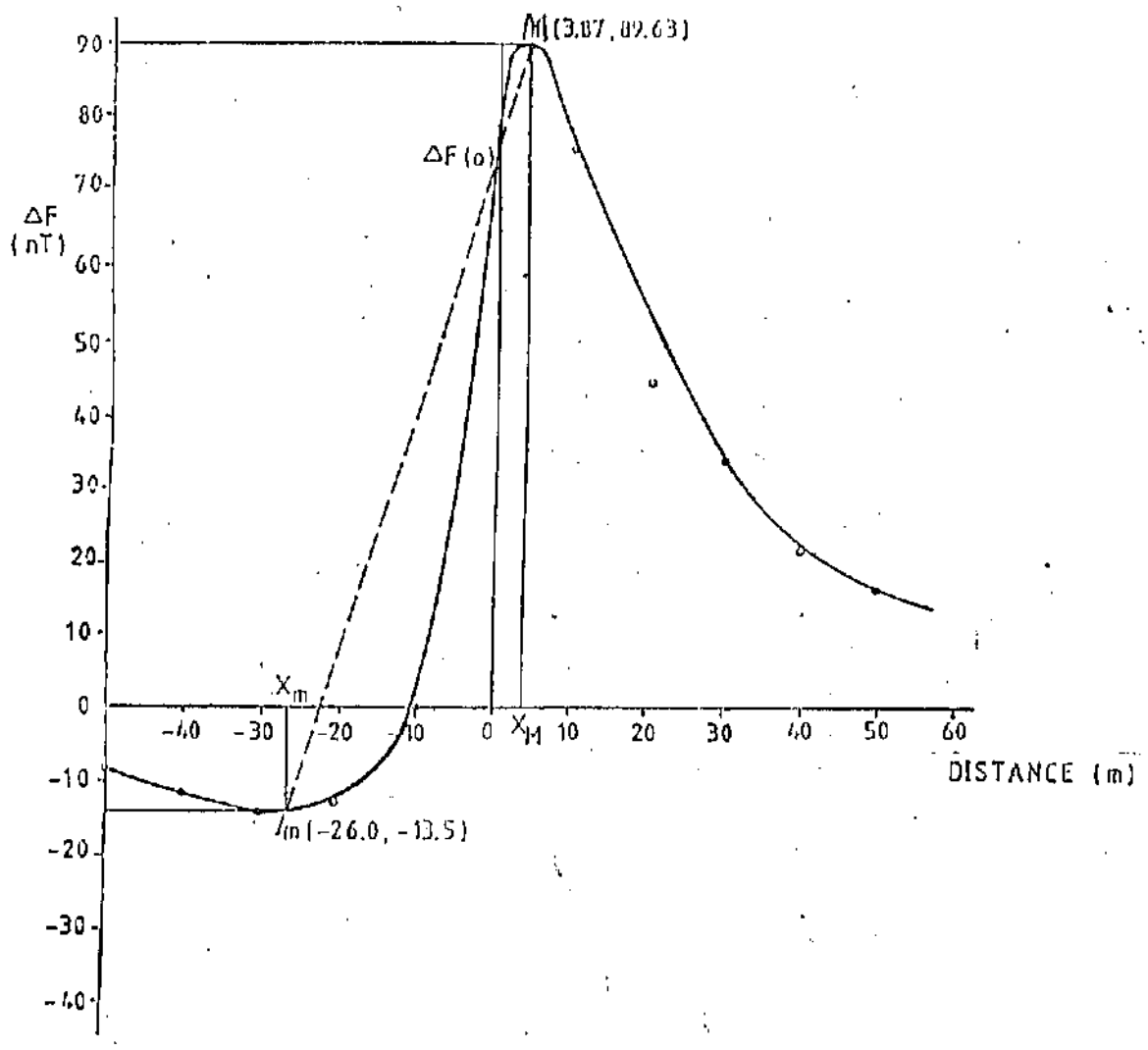


Fig 4.2 Diagrammatical Procedure For The Stanley's Method

1) The epicentral position and the baseline are determined previously for the Stanley's method.

2) Having completed step 1 above the next thing is calculating the Horizontal Gradient (ΔF_x) between the maximum and the minimum points of the anomaly. The gradient used in this work was calculated using a formula derived by Ku and Sharp (1983). The formula works for the total field data recorded in digital form and is given as follows

$$dTMAG(X)/dx = 0.0166667(TM7 - TM1)-0.15(TM6 - TM2) + 0.75(TM5 - TM3) \quad (4.1)$$

where TM1, TM2, TM3, TM5, TM6 and TM7 are the total field data recorded at six consecutive points respectively . Since this work involves large amount of data a simple computer program was written to execute this aspect of the work.

3) The value of the horizontal gradient at the epicentral position (x = 0) i.e (ΔF_x (0)) and at a position U (where $U = \sqrt{(|- X_m . X_M|)}$ i.e ΔF_x (U) are then read and used together with the known values of X_m, X_M and U in equation (3.36) to estimate the parameter θ_F

4) The parameter estimated above is then used with the known values of X_m and X_M to estimate the depth to the top of the source (h) using equation 3.30.

5) The parameter h estimated above is then used with known value of U to estimate the half width of the structure (b) using equation (3.32). The value b is then multiplied by 2 so as to obtain the full width of the structure.

6) The estimated parameters h, b, θ_F and U are then used in equations (3.27), (3.33) or (3.34) to estimate the value of the coefficient C_F.

7) The susceptibility contrast (χ) is then estimated with known value of C_F with the help of table 4.1.

The steps itemized above are illustrated in fig 4.3. It is worth mentioning that due to the number of anomalies interpreted in this work a computer program SPTDI.FOR was actually used to execute all the steps involved in both the Stanley's and the Pal's methods.

Table 4.1. The coefficients C_F and θ_F of equation 3.20

ΔF	C_F	θ_F
ΔZ	$2\chi F \sin\theta$	$I - \theta$
ΔH	$2\chi F \sin\theta \sin I$	$I - \theta - 90$
ΔT	$2\chi F \sin\theta \sin I \operatorname{cosec} I$	$2I - \theta - 90$

1) α, measured clockwise, is the angle that the dike's strike makes with the magnetic meridian (0 degree $\leq$ 180 degrees).

2) F and I are the strength and inclination (measured relative to the horizontal and reckoned positive downward) of the local geomagnetic vector respectively.

3) F' and I' are the effective strength and inclination respectively of the local geomagnetic vector in the direction of the profile and are computed using the relation : a) $I' = \tan^{-1}(\tan I \operatorname{cosec} \lambda)$; b) $F' = F \sin I \operatorname{cosec} I'$.

4) θ is the dip angle of the dike measured clockwise from the positive x-axis (0 degree $\leq \theta \leq$ 180 degrees).

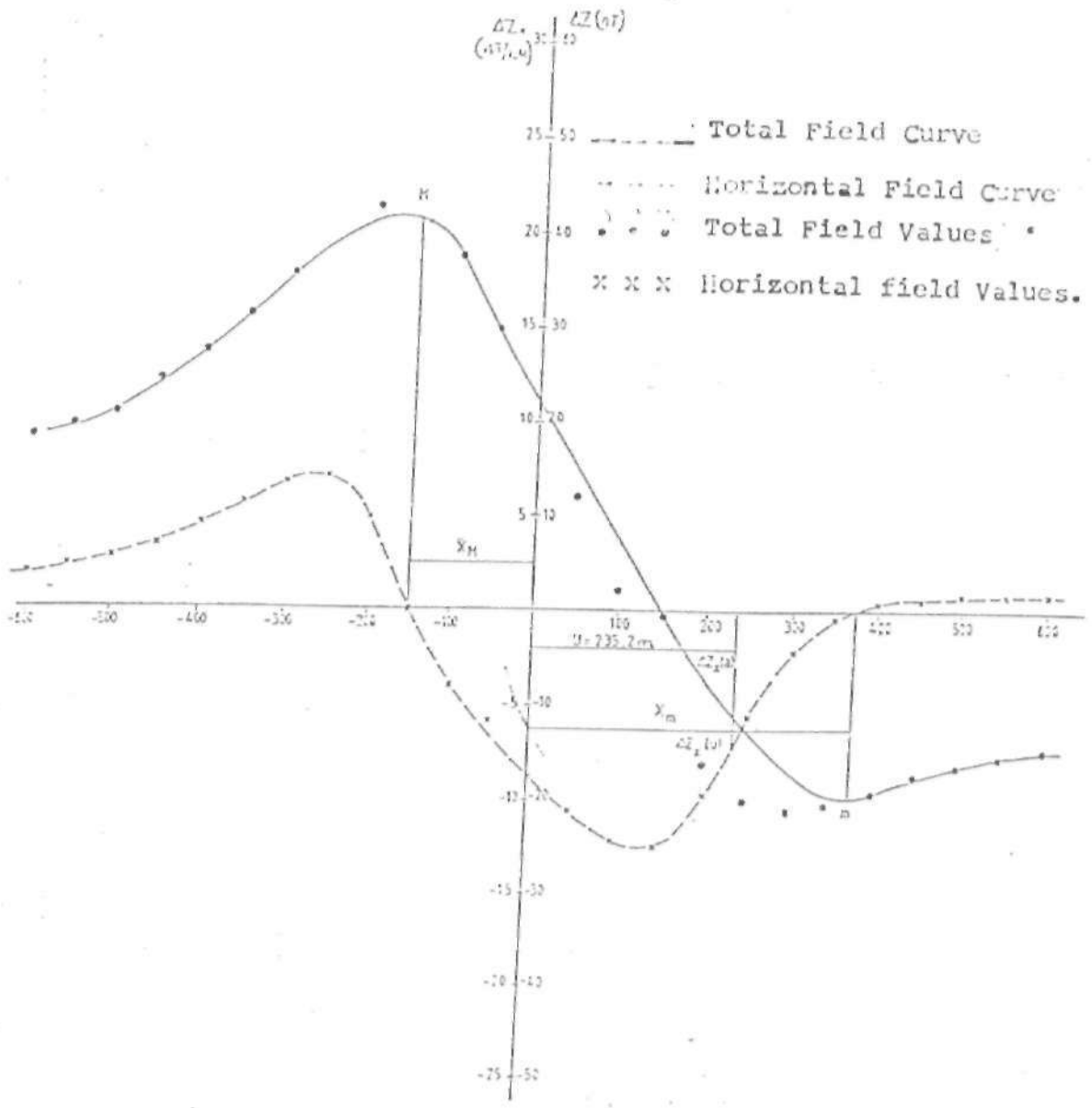


Fig 4.3 Diagrammatical Procedure For The Pal's Method

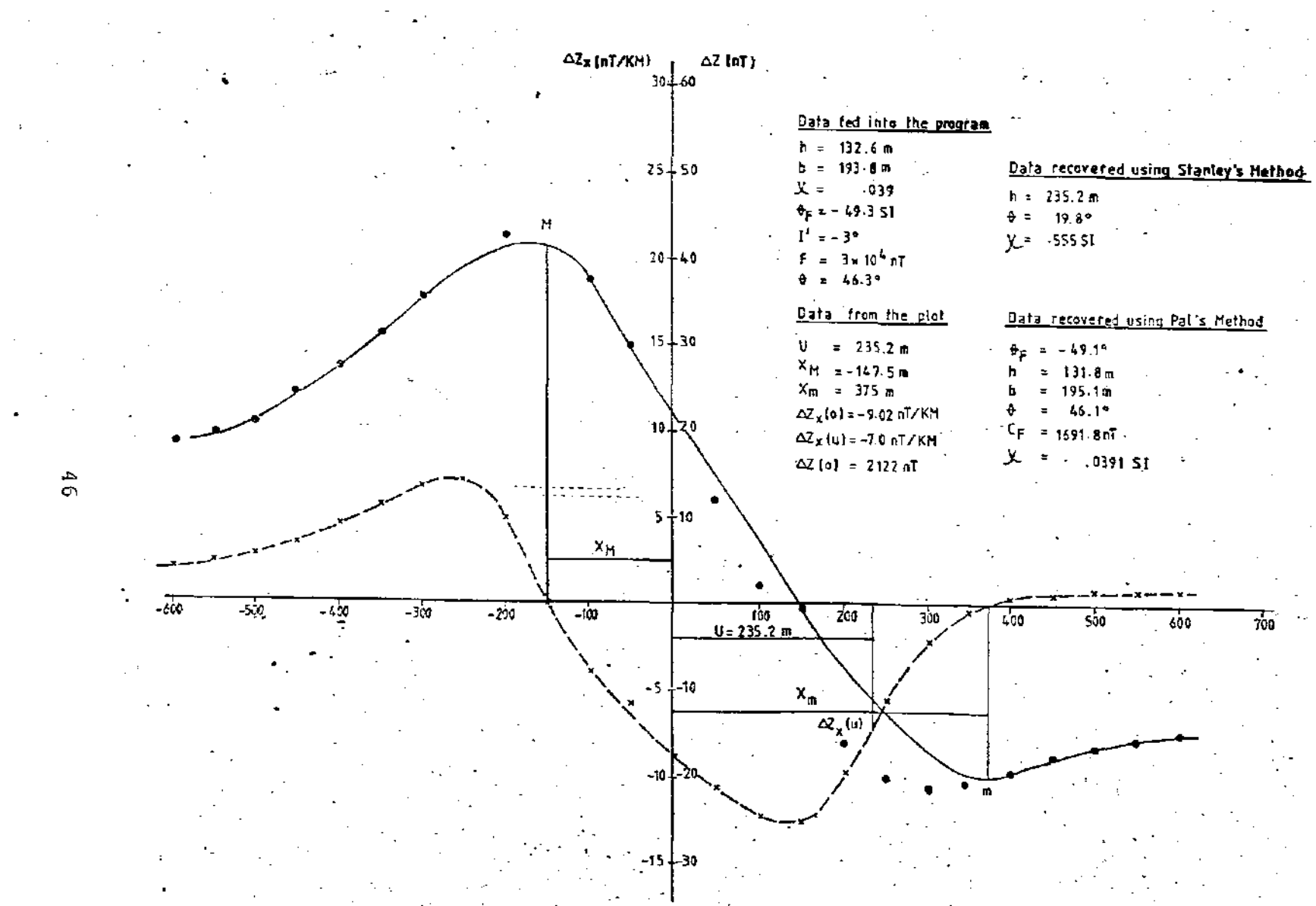
4.3.3 TESTING THE RELIABILITY OF THE INTERPRETATION TECHNIQUES

Prior to the typical interpretations of the anomalies of interest in this work a synthetic set of data was generated to ascertain the reliability of the two interpretation techniques. The equation of Gay (1963) was used to generate a hypothetical set of data using a computer program. All the values of the unknowns in the equation were supplied into the computer program. The anomaly obtained from this data was then interpreted using the Pal's method and the result is presented in fig 4.4. The same anomaly was then interpreted using the Stanley's method and the result is shown on fig 4.4.

4.3.4 COMPARISON OF THE RESULTS OBTAINED AFTER TESTING THE RELIABILITY OF THE INTERPRETATIONS TECHNIQUES

A close look at fig 4.4 shows that the depth estimates recovered using the Pal's method is in agreement with the value of the depth supplied into the program while the dip and the susceptibility contrasts estimates are also in agreement with the data supplied into the program respectively .

Also fig 4.4 also shows that the depth, width, and susceptibility contrast estimates recovered using the Stanley's method is not in good agreement with the parameters supplied into the program .



4.4 Diagram showing the Reliability Of The Interpretation Techniques

Table 4.2 Results obtained after the typical interpretations of the anomalies of interest.

		Pal's Method				Stanley's method		
Profile	Anomaly	Depth (Km)	Width (Km)	Dip	Sus. Contrast	Depth (Km)	Dip	Sus. Contrast.
L201	A1	0.47	2.54	-9.00	-0.0001980	0.59	- 5.7	-0.0043000
L202	A2	0.49	3.75	-45.3	-0.0000585	1.18	33.5	0.0018500
	A3	0.06	2.78	47.0	0.0000548	0.69	34.0	0.0006340
	A4	0.15	1.79	-29.9	-0.0001950	0.148	39.4	0.0000874
	A5	0.011	2.10	-1.8	0.0009440	0.29	- 8.1	-0.0005910
L203	A6	0.90	.44	-10.8	-0.0029300	0.37	17.4	0.0134000
	A7	0.46	2.85	35.7	-0.0000499	0.74	32.5	0.0006740
	A8	0.17	2.33	-9.6	0.0002760	0.42	- 6.5	0.0030000
L205	A9	1.29	2.28	32.2	0.0001340	0.91	36.2	0.0020400
L209	A10	0.72	2.05	36.6	0.0001980	0.49	40.1	0.0009560
L214	A11	0.54	2.97	18.6	0.0041600	0.82	2.79	0.2920000
L215	A12	0.028	2.44	21.1	0.0001290	0.30	10.70	0.0024100
	A13	- 0.092	2.89	-1.0	0.0002100	0.69	3.8	0.0048200
L216	A14	0.59	3.15	28.7	0.0002050	0.92	23.2	0.0036100
L218	A15	0.038	2.24	21.1	0.0001610	0.47	10.7	0.0038200
	A16	0.046	2.76	-29.3	-0.0002170	0.62	22.6	0.0021700
	A17	0.17	2.82	-8.0	0.0004190	0.71	5.7	-0.0220000
	A18	0.34	3.26	-12.5	0.0000566	0.91	30.3	-0.0006370
L219	A19	0.55	3.10	-42.6	-0.0001470	0.79	41.6	0.0020000
	A20	0.012	3.24	11.7	0.0000056	0.86	8.74	0.0077300
L220	A21	0.25	3.14	26.5	0.0001710	0.83	21.3	0.0027100
L222	A22	0.12	1.48	5.9	-0.0003470	0.00	3.72	-
	A23	0.063	2.42	43.6	0.0001560	0.45	34.9	0.0031600
L223	A24	0.29	2.35	-2.9	-0.0007870	0.34	3.7	0.0104200
	A25	0.44	3.53	40.9	0.0001410	1.06	29.8	00.0031800
	A26	0.53	3.04	-29.1	-0.0004600	0.85	23.4	.0060000
	A27	0.60	3.31	40.2	0.0000560	1.00	33.2	0.0034500
L225	A28	0.08	2.66	42.5	0.0000210	0.55	30.5	0.0011700
L226	A29	0.62	2.82	-30.0	-0.0002340	0.75	29.5	0.0027000

4.4 TYPICAL INTERPRETATIONS

In this work twenty nine anomalies were interpreted. These anomalies are labelled as A1, A2 , ..., A29

respectively The summary of the results obtained are given in table 4.2. However the detailed interpretation of only one these anomalies (anomaly A1 shown on fig 4.5) is here to illustrate the applications of each of the interpretation techniques used.

4.4.1 TYPICAL INTERPRETATION OF ANOMALY A1 USING THE PAL'S METHOD

The steps normally followed in interpreting anomalies based on the Pal's method are briefly described. As earlier mentioned the anomaly considered for this purpose is anomaly A1 shown on fig 4.5.

(1) The first step is to locate the epicentral position of the anomaly as described in section 4.3.2 and it was found out that X_M = 1.625 km and X_m = -1.125 Km respectively (fig 4. 5a)

(2) Thus U = 1.352 Km from equation (3.32), while $\Delta F_x(0)$ = - 2.7 nT/ Km and $\Delta F_x(U)$ = - 0.3 nT/kM respectively (from figure 4.5).

(3) Hence θ_F = -78.5 degrees and h = 0.47 Km from equations (3.36) and (3.30).

(4) Hence b = 1.27 Km from equation (3.32)

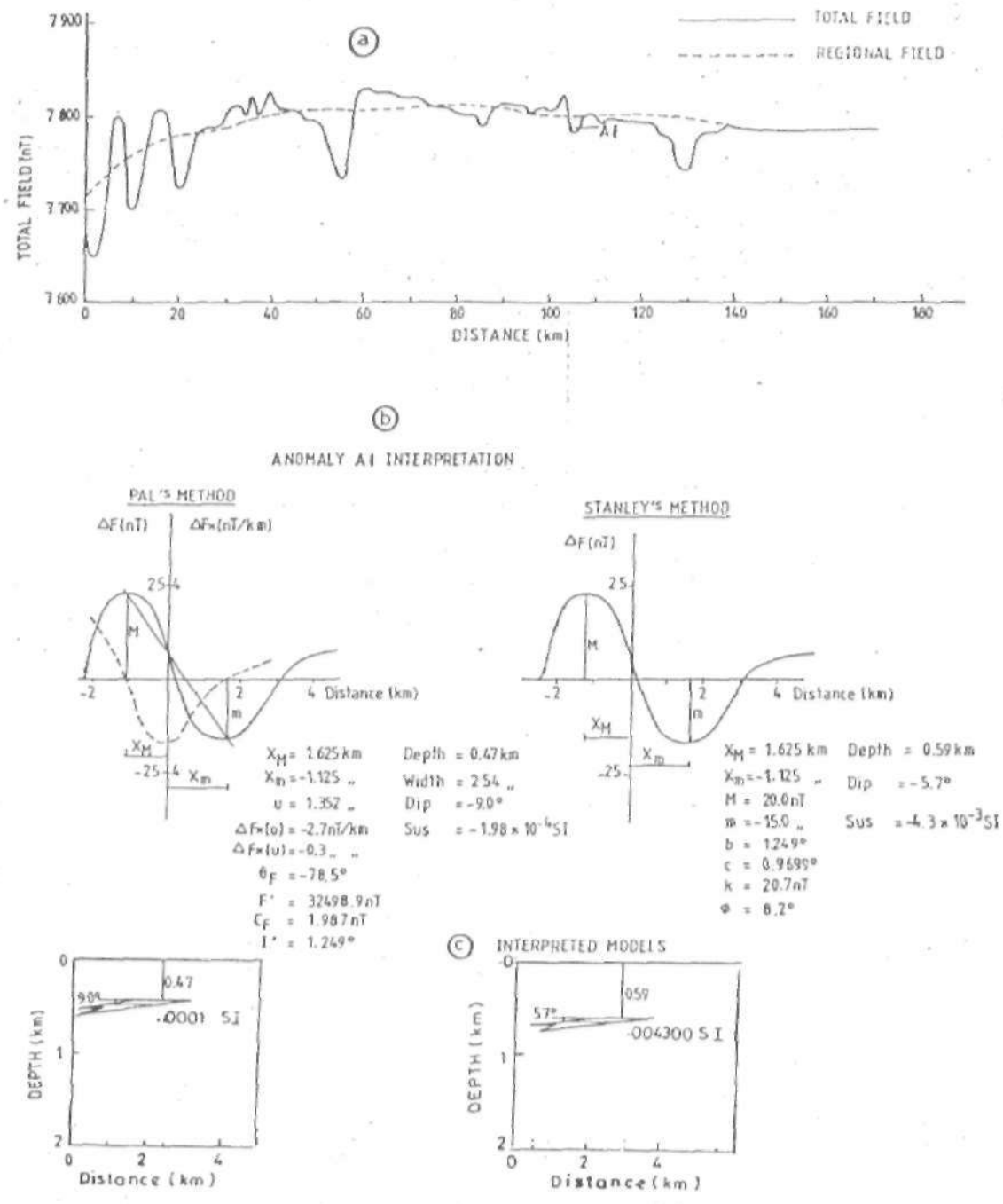


Fig.4.5. Interpretation of Anomaly A1 of profile L 201

(3) Hence θ_r = -78.5 degrees and h = 0.47 Km from equations (3.36) and (3.30).

(4) Hence b = 1.27 Km from equation (3.32)

(5) Equation (3.33) yields C_r = 1.249 nT. Thus χ = - 0.000198 (SI)from table 4.2 and when I' = 1.249 degrees and F'= 32498.9 nT.

(6) Thus α = -9.0 degrees from table 4.1

4.4.2 TYPICAL INTERPRETATION USING THE STANLEY'S METHOD.

Similarly the steps followed in interpreting anomalies based on the Stanley's method are briefly described below. As earlier mentioned the anomaly considered for this purpose is anomaly A1 shown on fig 4.5.

(1) The first step is to locate the epicentral position and the baseline respectively as described in section 4.3.2.

(2) Hence X_M = 1.625 Km , X_m = - 1.125 Km , m = - 15.0 nT and M = 20.0 nT respectively (figure 4.6b).

(3) Thus ϕ = -8.2 degrees from equation (3.15) , and α = - 5.7 degrees from equation (3.1a) when b = 1.249 and the depth (d) = 0.59 Km from equation (3.19) respectively.

(4) Hence K = 20.7 nT from equation (3.15) and χ = - 0.0043 (SI) from equation 3.1f when C = 0.969.

5 SUMMARY OF THE FINDINGS OF THE PRESENT WORK.

A close inspection of table 4.2 indicates that according to the interpretation based on the Stanley's (1977) method the igneous intrusions causing the aeromagnetic anomalies of interest are at depths between 0.00 Km and 1.29 Km. The table also shows that majority of the igneous intrusions are associated with high positive susceptibility contrasts which ranges between 1.17×10^{-3} SI and 2.92×10^{-1} SI while a few of them are associated with low positive susceptibility contrasts of between 8.74×10^{-5} SI and 9.56×10^{-4} SI and also negative susceptibility contrasts ranging between -6.37×10^{-4} SI and -2.2×10^{-2} SI respectively. The table also shows that interpretations based on the Pal's method has shown that the igneous intrusions causing the anomalies are buried at depths between 0.011 Km and 1.18 Km. The table also shows that the majority of the igneous intrusions causing the short wavelength of interest are associated with low positive magnetic susceptibility values which ranges between 5.48×10^{-5} SI and 5.60×10^{-4} SI while few of them are associated with high positive susceptibility contrasts which ranges between 4.16×10^{-3} and 4.19×10^{-3} and negative susceptibility contrasts respectively ranging between -5.85×10^{-5} and -2.93×10^{-3}.

CHAPTER FIVE

DEDUCTIONS, CONCLUSIONS AND RECOMMENDATIONS

5.1 DEDUCTIONS

5.1.1 COMPARISON OF THE TWO SETS OF INTERPRETATIONS

It could be seen from table 4.2 that the depth estimates given by the two methods except for a few cases are not in fair agreement with one another. However, the maximum depth to the top of the causative bodies (1.18 Km by the Pal's (1985)) method and 1.29 Km for the Stanley's (1977) method) are in agreement with one another. The dip estimates and the susceptibility contrasts given by the two interpretation techniques are not in good agreement with one another. However, it is noticeable that the susceptibility contrasts given by the Stanley's (1977) method is consistently greater than those given by the Pal's (1985) method by a factor of 10. The reasons for the disagreement could probably be due to the fact that both methods are using different models for their interpretations. The different basic assumptions put forward to arrive at the expressions for source parameters make the values of the source parameters obtained from these expressions to be different. Furthermore, Ku and Sharp (1983) have shown that both dip and susceptibility estimates are dependent on the thickness of dike bodies, therefore, since the thickness of thin dikes is less than that of thick dikes then the estimates of the dip and susceptibility will be different.

Generally estimates obtained from these graphical techniques are better utilised if used as initial parameters for methods such as spectral analysis and inverse modelling techniques.

5.1.2 GEOLOGICAL IMPLICATIONS OF THE INTERPRETATIONS

The Stanley's (1977) method has suggested three sets of ranges for the sub-surface intrusions in the study area (table 4.2), these are those with high magnetic susceptibility contrasts (between 1.17×10^{-3} and 2.92×10^{-1}), low positive susceptibility contrasts (between 8.74×10^{-5} and 9.56×10^{-4}) and negative susceptibility contrasts of range between -6.37×10^{-4} and -2.2×10^{0}. The intrusions associated with the high magnetic susceptibility contrasts are thought to be due to basalts as suggested by Telford et. al, (1976). Thus, this suggests the presence of basalts at depths between 0.3 and 1.18 km in the study area. The presence of basalts on the surface of Biu plateau to the SW of our study area have earlier been reported by Tokarski (1973). Also the low positive range of magnetic susceptibility contrasts found in the study area are thought to be due to granites as suggested by table 5.1. This, then implies the presence of granites at depths between 0.148 and 0.74 km in the study area.

Table 5.1 (a): Suggested range of depths and susceptibility contrasts of the modeled Igneous intrusions in the study area

Depth (km)	Susceptibility Contrast (SI)	Suggested rock type	Graphical Method used
0.3-1.18	1.17×10^{-3} - 2.92×10^{-1}	Basalts	Stanley's
0.148-0.74	8.74×10^{-5} - 9.56×10^{-4}	Granites	Stanley's
0.29-0.91	-6.37×10^{-4} - (-2.2×10^{-2})	Acidic Rocks	Stanley's
0.17-0.54	4.16×10^{-3} - 4.19×10^{-3}	Basalts	Pal's
0.011-1.29	5.48×10^{-5} - 5.6×10^{-4}	Granites	Pal's
0.046- 0.9	-5.85×10^{-5} - (-2.93×10^{-3})	Acidic Rocks	Pal's

Table 5.1 (b): Susceptibilities of some rock types (Source: Telford et al, 1976)

Type	Susceptibility range x 10^{-6}
Granites	0 - 4000
Basalts	20 - 14,500

Negative susceptibility contrasts implies associations with acidic rocks containing minerals such as silica (Dobrin, 1976) Therefore the existence of intrusions with negative susceptibility contrasts in the study area implies the potentiality of the occurrence of minerals such as silica in the study area. Finally, the interpretations based on this method in this work have suggested that basalts are the predominant rock types in the study area.

The Pal's (1985) method has suggested three sets of ranges for the sub-surface structures in the study area (table 4.2), these are those with high magnetic susceptibility contrasts (between 4.16×10^{-3} and 4.19×10^{-3}), low positive magnetic susceptibility contrasts (5.48×10^{-5} and 5.60×10^{-4}) and negative susceptibility contrasts ranging between -5.85×10^{-5} and -2.93×10^{-3} SI.

As mentioned above these ranges suggests the presence of basalts, granites and acidic rocks in the study area. The method suggests that granites are the predominant rock types in the area. However, geological evidences from the work of Tokarski (1973) has suggested that basalts are the predominant rock types in the area, hence based on this, interpretations based on the Stanley's method are thought to be more plausible in this work.

Finally, it could be seen from table 4.2 that the two interpretations based on the two techniques used in this work techniques suggested that some of the modeled intrusives are lying at shallow depths which implies the presence of lava flows. The existence of these lava flows and the basaltic intrusions suggests an occurrence of volcanic activity in the study area. The volcanic rocks must have ascended to these depths as a result of rifting at the basement through which they rise upward as molten magma and later solidified at the shallow depths after cooling. This further suggests that either the Chad Basin has a rift origin similar to the adjacent Benue trough or the adjacent Benue trough has extended through the Chad Basin.

5.3 CONCLUSIONS

The major conclusions that could be drawn from this study can be itemized as follows;

1) The present work has revealed that the short wavelength anomalies of interest in this work are caused by three types of igneous intrusions namely basalts, granites and acidic rocks. Suggestion from the interpretations based on the Stanley's (1977) method

(which was supported by the geological work of Tokarski (1973)) which has hinted that basalts are the predominant rock types in the study are was adopted. Therefore, basalts are thought to be the predominant rock types in our study area. It is also worth mentioning that apart from the presence of basalts and gabbro hitherto mentioned by previous works, this work has revealed the existence of acidic rocks in our study area. The occurence of the acidic rocks is suggestion for the potentiality of having minerals such as silica in the study area.

2) The work has also revealed that the short wavelength anomalies of interest are lying between the depths of 0.148 and 1.18 km. Though the task of determining the thickness of the sediments goes beyond the scope of this work, however the work of Ajayi and Nkereuwem (1992) has suggested that the maximum depth to basement in the study area is 4 km. Based on this, one can suggest that all the modeled intrusives are lying within the sediments. This is agreement with the work of Ajayi and Nkereuwem (1992).

3) The present work has revealed that some of the modeled intrusive are lying at shallow depths which was interpreted to be lava flows. The presence of the lava flows and the basaltic intrusions suggested a rifting origin for the study area. This further suggests that either the Chad basin has a rift origin or that the adjacent Benue trough has extended through the Chad basin.

5.4 LIMITATIONS OF THE PRESENT WORK

(1) To the best knowledge of the author no previous work has been undertaken to interpret the short-wavelength anomalies considered in this study, hence comparison of the results of this work with any past work is not possible.

(2) As the source of the data used in this work originates from aeromagnetic survey, the author has no control on the quality of the data used.

5.5 SUGGESTIONS FOR FUTURE WORK

To throw more light on the Chungowa depression , a ground gravity and magnetic surveys to cover the study area should be carried out so as to confirm the existence of the aeromagnetic anomalies considered in this study. Also, both 2-D and 3-D iterative modelling techniques should be used to map the causative bodies in greater detail. Finally, methods such as spectral analysis and Werner deconvolution technique should be used to study the geometry of the entire Chad basin.

REFERENCES

Affleck, J. (1963). Magnetic anomaly trends and spacing patterns. Geophysics 28, 379 - 395.

Ajakaiye, D. E. and Burke K. (1972). A Bouguer gravity map of Nigeria. Tectonophysics Vol. 16, Page 103 - 115.

Ajayi, C.O and Nkereuwem (1992). Determining the Location of the intra - sediment igneous intrusions and basement structure in the Chungowa Depression, Chad Basin, Nigeria, *from aeromagnetic data. A paper presented at the 28th N.M.G.S. annual* conference, Port - Harcourt.

Barber, W. (1965). Pressure Water in the Chad Formation of Bornu and Dikwa emirates North - Eastern Nigeria. Geological Survey Nigeria Vol 35, p 5 - 20.

Barber, W. and Jones, D.G. (1960). The Geology and Hydrology of Maiduguri, Bornu Province. Rce. Geological Survey Nigeria.
Vol 30, p 109.

Cratchley, C.R. (1960). Geophysical Survey of the South - Western part of the Chad Basin C.C.T.A.

Dobrin, M.B. (1976). Geophysical prospecting, 2nd Edition New York, McGraw - Hall Publishers Inc.

Durotoye, B. (1976). Quaternary sediments in Nigeria. In Geology Of Nigeria, C.A. Kogbe (ed), Elizabethan Publishing Co. Lagos.

Furon, R. (1963). The Geology of Africa, Oliver and Boyd, Edinburgh, London, 377pp.

Gay, S. P. (Jr) (1963). Standard curves for interpretation of magnetic anomalies over long tabular bodies. Geophysics 28, pp. 161 - 200.

Grant F. S. and West, G.F. (1965). Interpretation Theory in Applied Geophysics, McGraw - Hall Publishers Inc.

Howell, D. F (Jr). , 1969. Introduction to Geophysics, McGraw - Hill, London.

Johnson, W. W (1969). A Least Squares method of Interpreting Magnetic Anomalies Caused by Two - Dimensional Structures. Geophysics 34, 65 - 74.

Ku, G .C. and Sharp, J.A. (1963). Werner Deconvolution for automated magnetic interpretation and its refinement using the Maquardts inverse modelling. Geophysics 48, pp 754 - 774.

Matheis, G. (1976). Review of the Geology of the Chad Basin in Nigeria in Geology of Nigeria, edited by C. A. Kogbe, pp 287 - 294, Elizabethan Publishing company, Lagos.

Nettleton, L.L. (1940). Geophysical Prospecting For Oil. McGraw - Hall, New York.

Pal, P.C. (1985). A gradient analysis - based simplified strategy for the magnetic anomaly of an inclined and infinite thick dike. Geophysics Vol. 50. pp 1179 - 1182.

Reyment, R.A. (1956). On the Stratigraphy of the Cretaceous of Nigeria and Cameroon, British West Africa. Geol Foren Stockh, Fort, 78, p 17 - 96.

Reyment, R.A. (1965). Aspects of the Geology of Nigeria. University of Ibadan Press, 145 pp.

Stanley, J.M. (1977). Simplified Magnetic Interpretation of the Geological Contact and a thin dike. Geophysics 42,
pp 1236 - 1240.

Telford, W.M. Geldart, L.P. Sheriff, R.E and Keys D.A. (1973). Applied Geophysics, Cambridge University Press.

Tokarski, A. (1973). Geological Possibilities Of Chad Oil in Nigeria. Occasional Paper No. 3. Department of Geology A.B.U. Zaria.

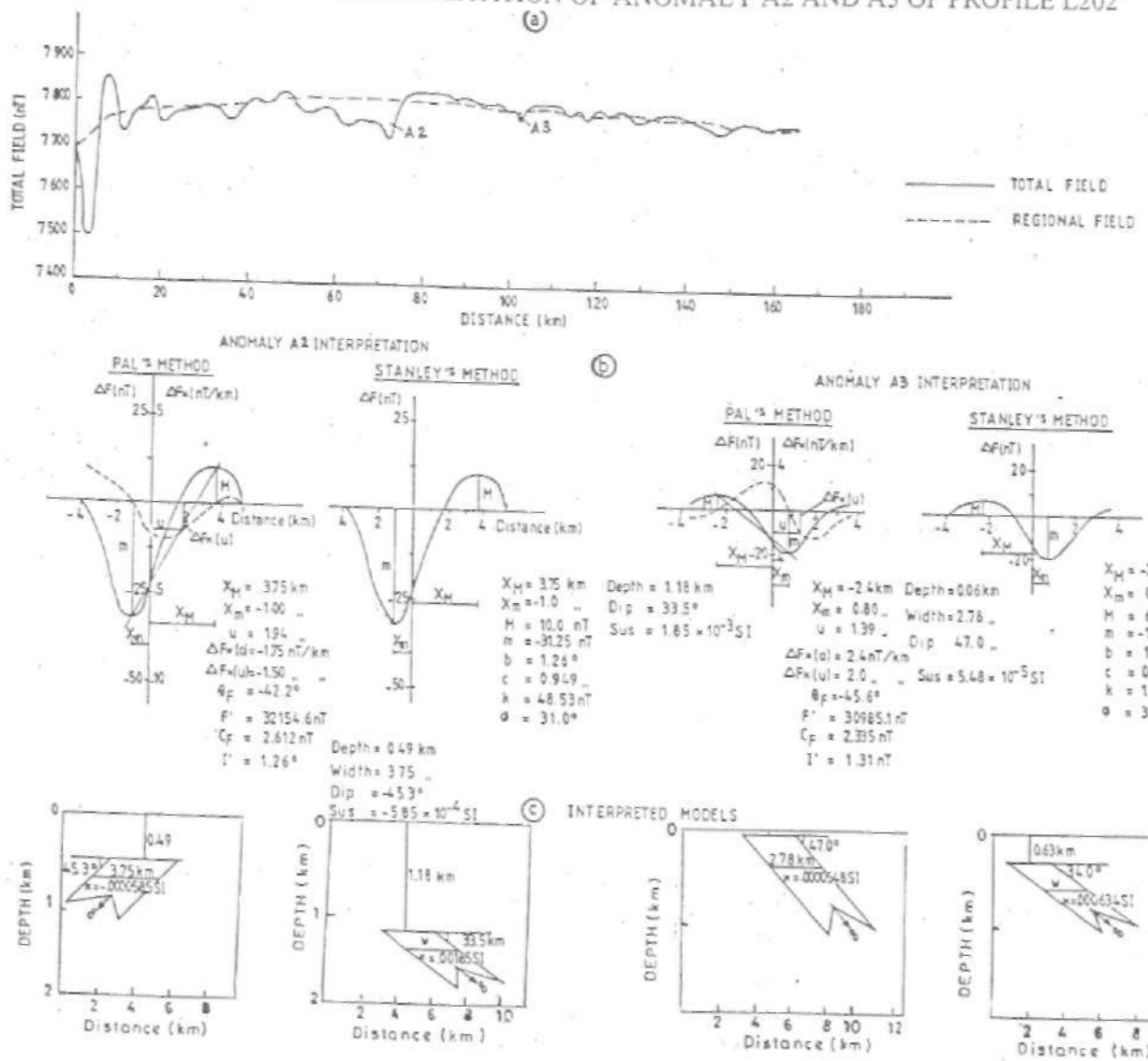
Turner, D.C. (1971). The Sedimentary Cover in Nigeria, in Tectonics of Africa. UNESCO Publication. pp 403 - 405.

Vacquier, T. S, N.C Henderson R.O and Zeity .I. (1951). Interpretation of Aeromagnetic maps. Geological Society, A.M.Mene 47.

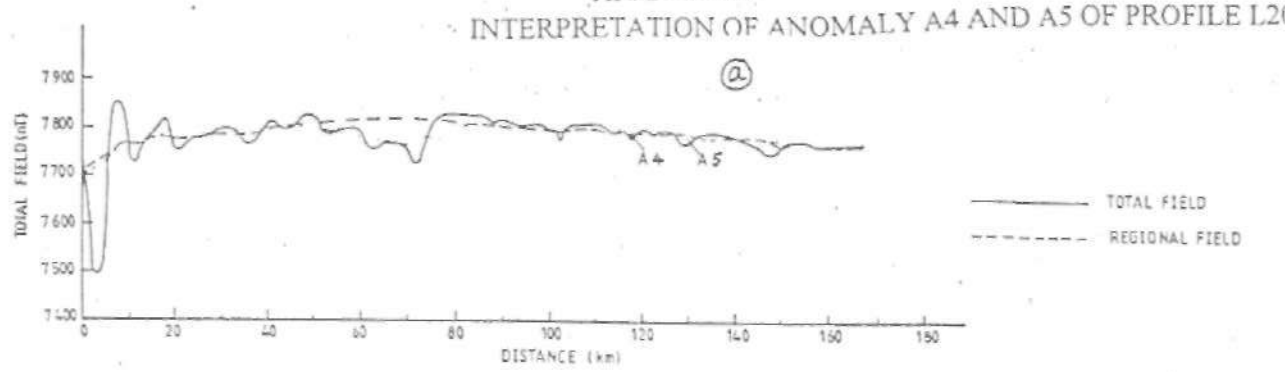
Won, I.T (1981). Application of Gauss's method to Interpretation of magnetic anomalies of Dipping dikes. Geophysics 46, 211 - 215.

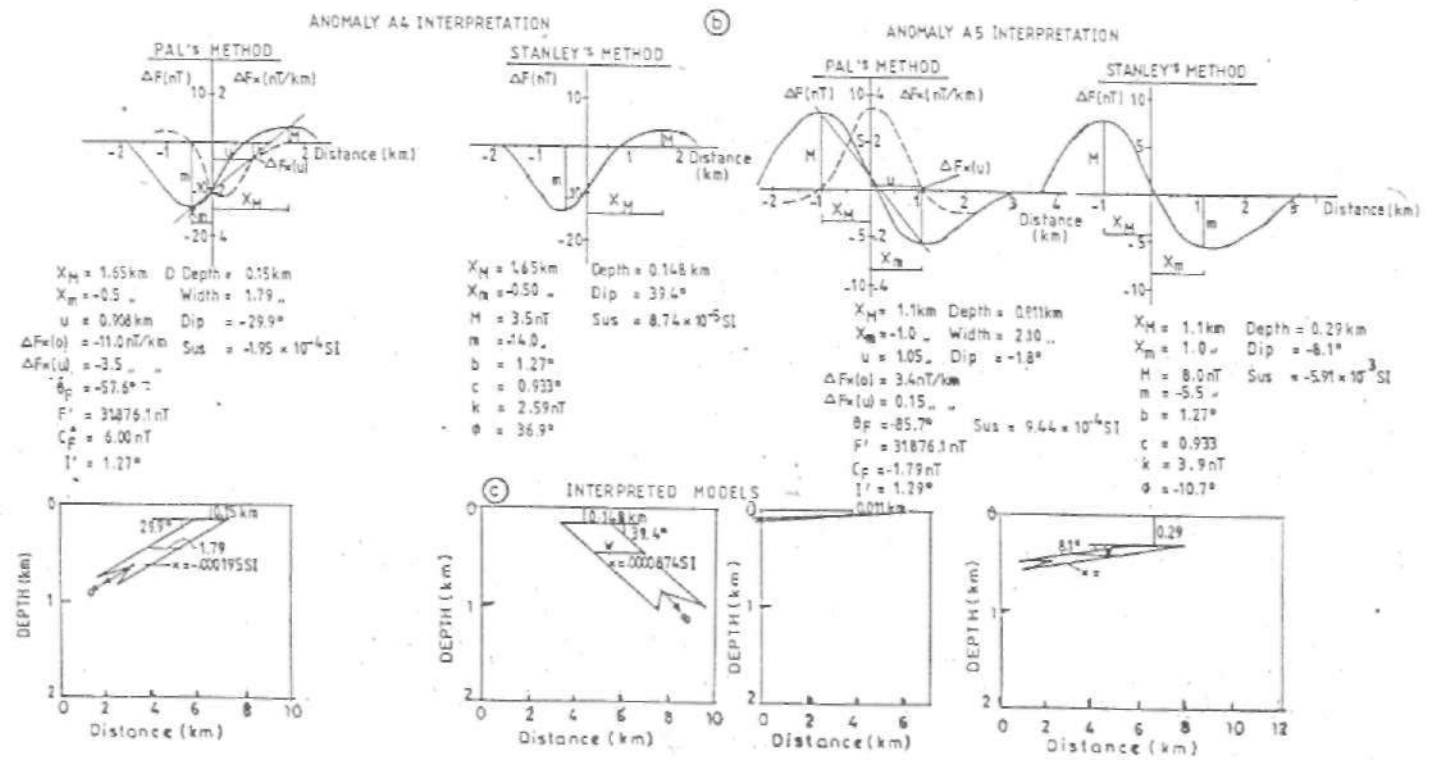
Yusuf, L. (1990). Werner Deconvolution and Interpretation of Aeromagnetic data over parts of the Upper Benue Trough, Nigeria. Unpublished Msc Thesis A.B.U. Zaria.

APPENDIX I
INTERPRETATION OF ANOMALY A2 AND A3 OF PROFILE L202



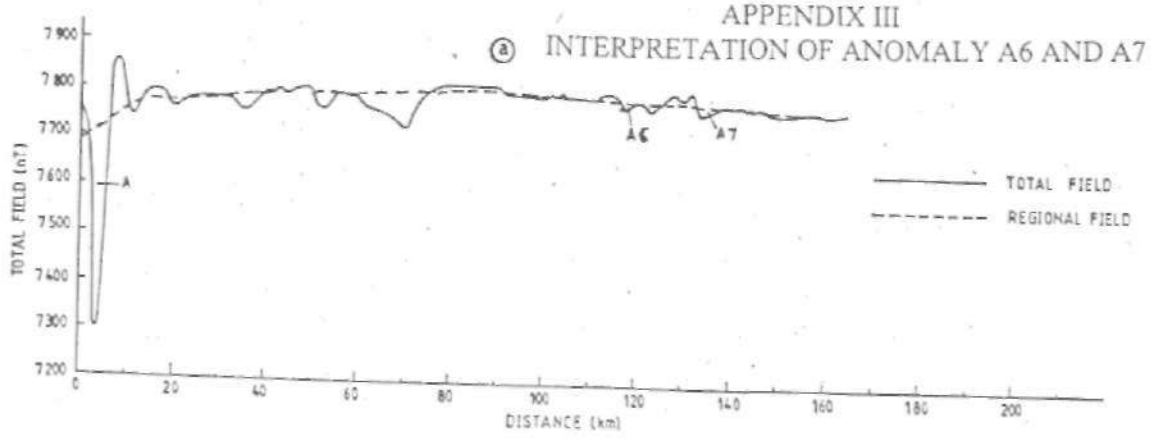
APPENDIX II
INTERPRETATION OF ANOMALY A4 AND A5 OF PROFILE L202

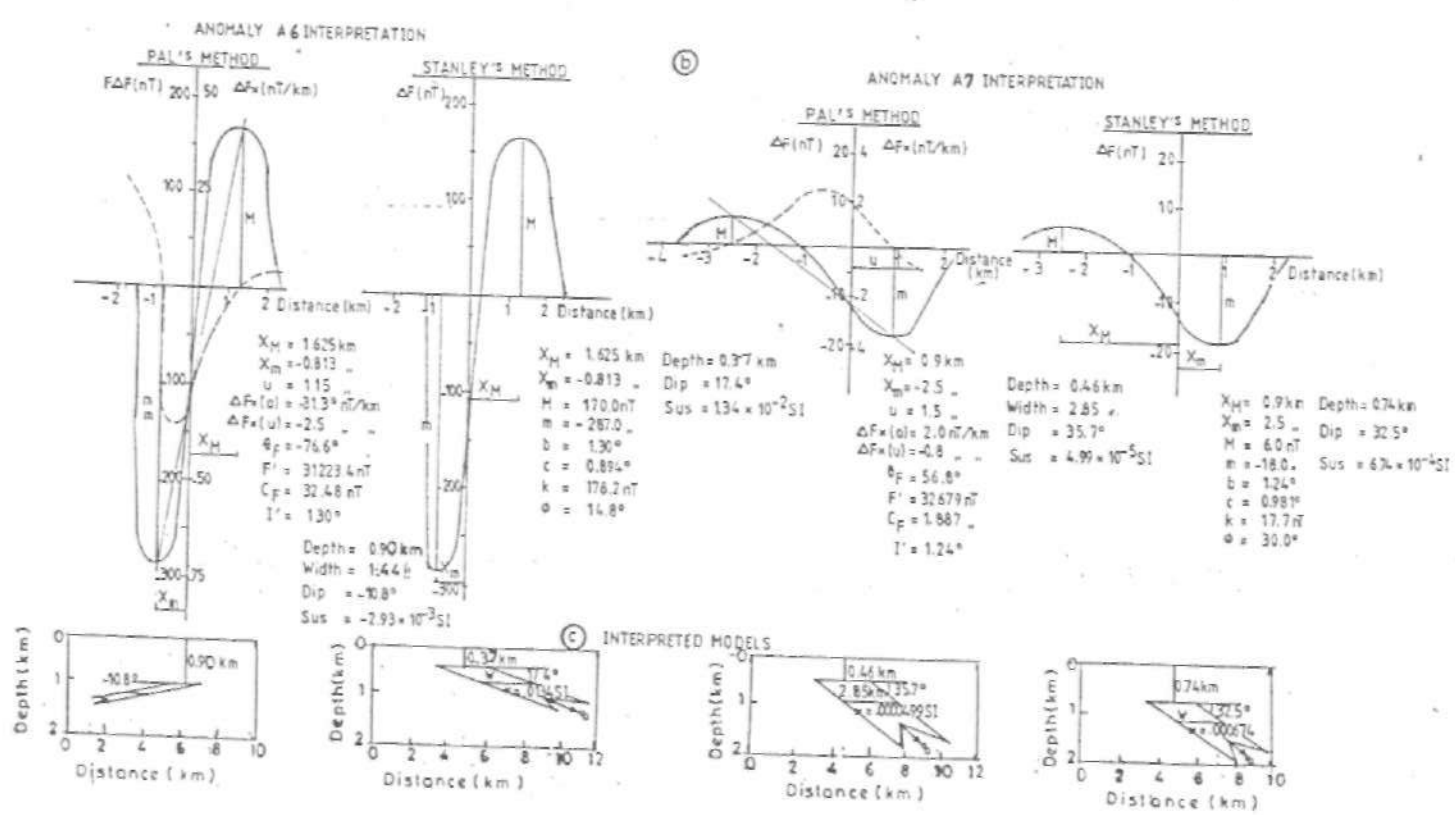




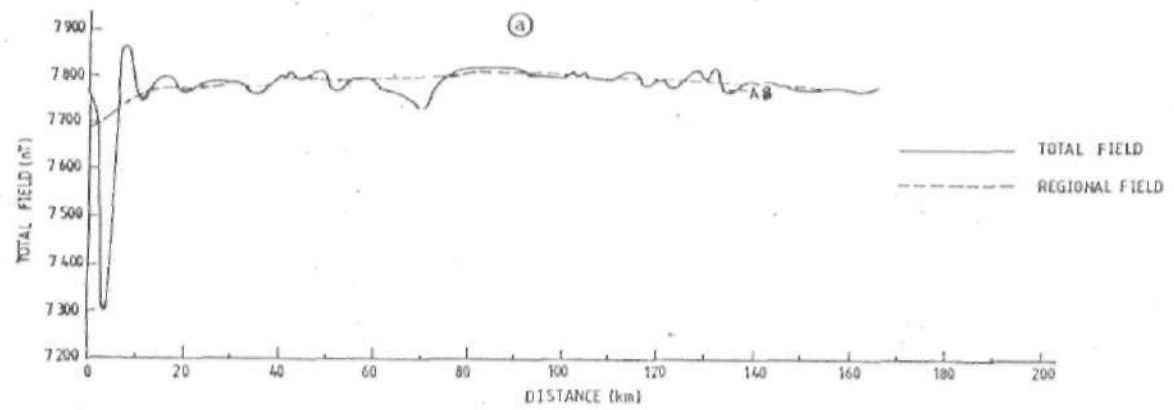
APPENDIX III

ⓐ INTERPRETATION OF ANOMALY A6 AND A7 OF PROFILE 203

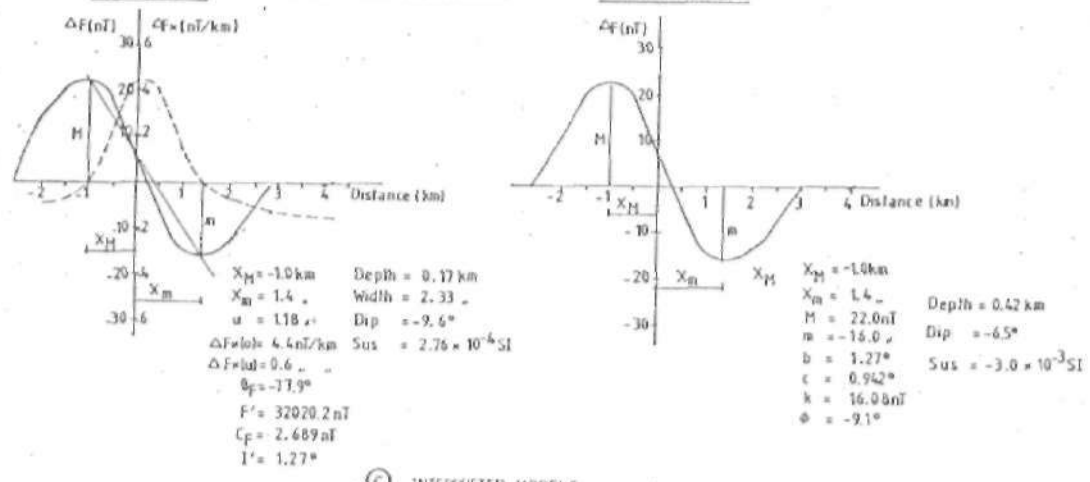




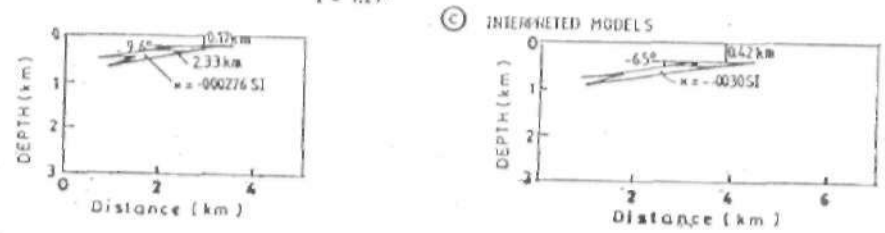
APPENDIX IV
INTERPRETATION OF ANOMALY A8 OF PROFILE L203



ⓑ ANOMALY A8 INTERPRETATION

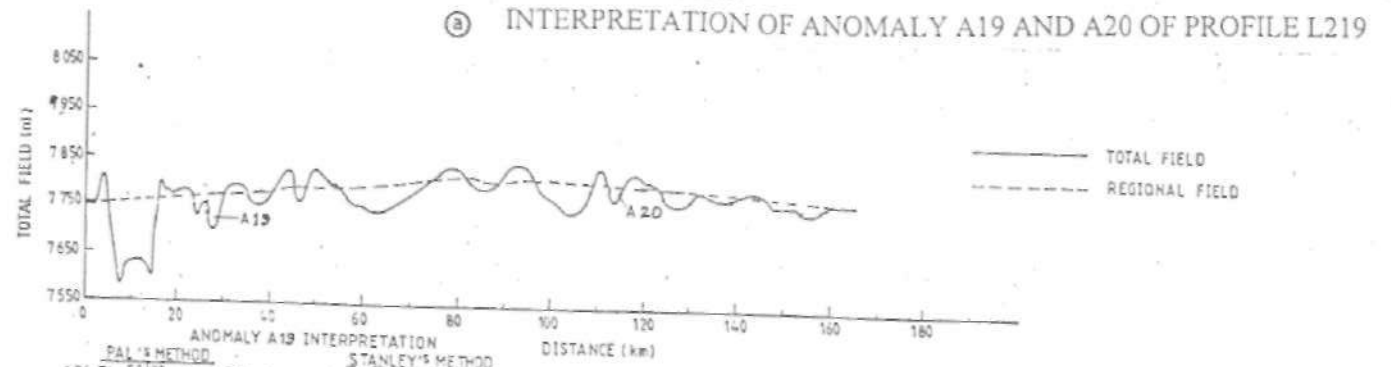


ⓒ INTERPRETED MODELS

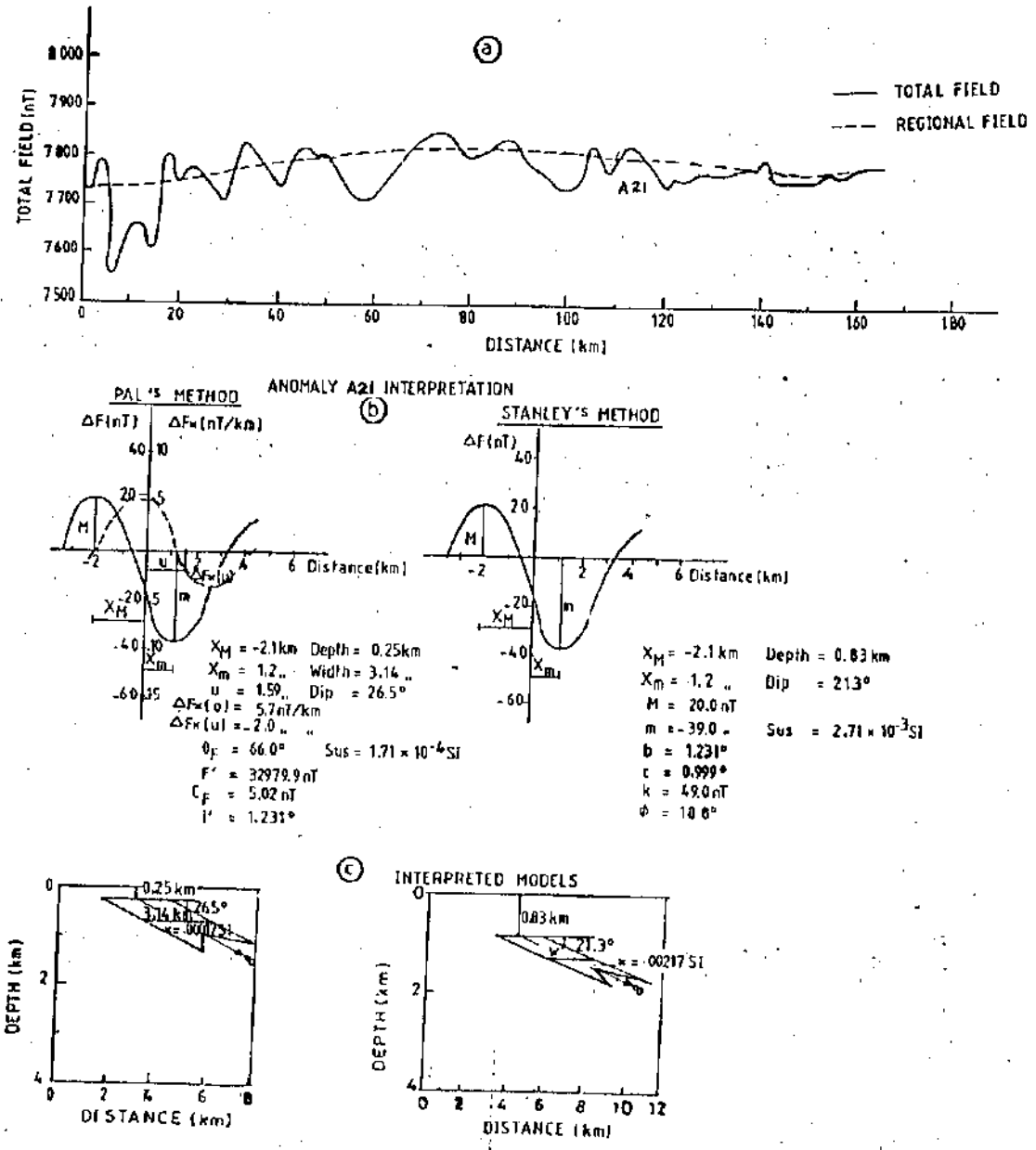


APPENDIX VI

ⓐ INTERPRETATION OF ANOMALY A19 AND A20 OF PROFILE L219

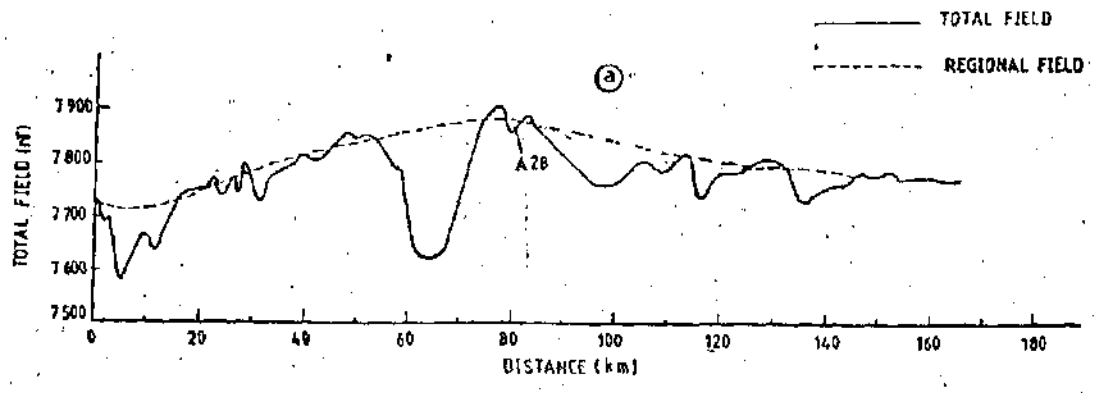


APPENDIX VII
INTERPRETATION OF ANOMALY A21 OF PROFILE L220

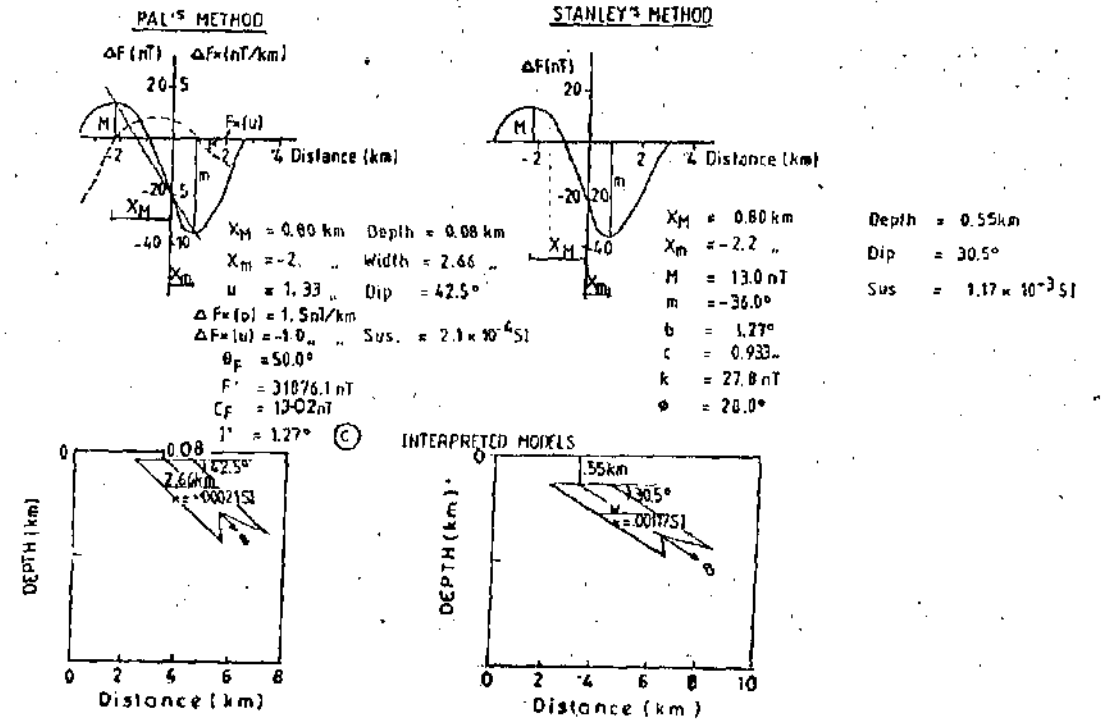


APPENDIX VIII

INTERPRETATION OF ANOMALY A28 OF PROFILE L225



(b) ANOMALY A28 INTERPRETATION



APPENDIX IX
INTERPRETATION OF ANOMALY A29 OF PROFILE L226

